Université de Montréal

Assessing neural network dynamics under normal and altered states of consciousness with MEG: Methodological challenges and proposed solutions for atypical power spectra

par

Timothy Nest

Département d'informatique et de recherche opérationnelle
Faculté des arts et des sciences

Mémoire présenté en vue de l'obtention du grade de
Maître ès sciences (M.Sc.)
en Informatique

October 27, 2021

Université de Montréal

Faculté des arts et des sciences

Ce mémoire intitulé

Assessing neural network dynamics under normal and altered states of consciousness with MEG: Methodological challenges and proposed solutions for atypical power spectra

présenté par

Timothy Nest

a été évalué par un jury composé des personnes suivantes :

Irina Rish
(président-rapporteur)

Karim Jerbi
(directeur de recherche)

Pierre Bellec
(codirecteur)

Guillaume Dumas
(membre du jury)

Résumé

Cette dernière décennie a vu un certain nombre d'avancées significatives en mathématiques, en apprentissage computationnel et en traitement de signal, qui n'ont pas encore été pleinement exploitées en neurosciences. En particulier, l'évaluation de la connectivité dans les réseaux neuronaux peut grandement bénéficier de ces travaux. Nous proposons ici d'exploiter ces outils pour combler partiellement le fossé considérable qui existe encore entre la recherche connectomique à grande échelle (largement centrée sur des mesures indirectes de l'activité cérébrale comme l'Imagerie par résonance magnétique fonctionnelle (IRMf)) et les mesures physiologiques plus directes de l'activité cérébrale. Il est particulièrement important de combler ce fossé pour l'étude des propriétés physiologiques associées à divers états de conscience normaux et anormaux, notamment les troubles psychiatriques, le sommeil, l'anesthésie ou les états induits par les drogues. Les travaux récents sur l'induction d'états de conscience altérés par des agonistes non sélectifs de la sérotonine, tels que la psilocybine et le Diéthyllysergamide (LSD), en sont de bons exemples.

Au cours des cinq dernières années, une résurgence rapide de la recherche sur la neurobiologie des tryptamines psychédéliques s'est produite, après une interruption d'un demi-siècle. Bien que ces substances présentent un grand potentiel pour éclairer des aspects jusqu'ici non interrogés du fonctionnement normal et anormal du cerveau, l'ampleur et le caractère inhabituel des changements qu'elles provoquent posent de sérieux défis aux chercheurs. La découverte de méthodes convaincantes et évolutives pour étudier ces données est d'une grande importance si nous voulons tirer parti de la fenêtre unique que ces substances atypiques offrent sur les aspects centraux de la conscience et des fonctions cérébrales anormales. Dans la présente thèse, nous résumons l'état actuel de la neuro-imagerie électrophysiologique en ce qui concerne l'étude des tryptamines psychédéliques, et nous démontrons un certain nombre de lacunes évidentes dans la recherche électrophysiologique actuelle sur les psychédéliques. Nous offrons également quelques modestes contributions méthodologiques au domaine. L'utilité de ces contributions est soutenue par quelques résultats empiriques intrigants, bien que préliminaires. Dans le premier chapitre, nous présentons l'histoire de la recherche neuroscientifique sur le LSD. Il a été rapporté que le LSD induit des déplacements de pics dans les spectres de puissance, en même temps que des diminutions de l'amplitude

des pics. Le fait que ces effets soient liés entre eux et que la plupart des recherches menées jusqu'à présent n'aient pas cherché à les distinguer est uniformément négligé dans la littérature, ce qui, selon nous, peut conduire à de fausses interprétations.

Le chapitre 2 examine certains des avantages plausibles ainsi que les obstacles sérieux à la recherche sur la connectivité du cerveau entier par magnétoencéphalographie (MEG), et propose plusieurs stratégies pour surmonter ces limites méthodologiques. Celles-ci comprennent des stratégies d'imagerie de source convaincantes, des développements nouveaux et récents dans la décomposition spectrale, des mesures de connectivité insensibles à la conduction volumique, et des implémentations évolutives de métriques de couplage interfréquence bien établies. Nous montrons que ces techniques peuvent être étendues à une grille corticale et sous-corticale de plus haute résolution que celle qui existe actuellement. Nous discutons également d'une mise en œuvre allégée de statistiques non paramétriques adaptées à ces données. Le troisième chapitre a pour but de démontrer l'efficacité de ces procédures, en montrant les résultats empiriques d'une étude de la connectivité du cerveau entier sous LSD par MEG. Le quatrième et dernier chapitre discute de ces résultats, ainsi que des précautions nécessaires et des orientations futures prometteuses pour ce type de recherche. Il propose des approches computationnelles supplémentaires qui pourraient étendre la portée de ces recherches et, plus généralement, de l'électrophysiologie du cerveau entier. Dans l'ensemble, le cadre méthodologique proposé dans ce travail surmonte les limitations endémiques précédentes, non seulement dans la recherche sur les psychédéliques, mais aussi dans la recherche électrophysiologique en général, et jette une lumière nouvelle sur sur les mécanismes centraux qui sous-tendent ces états de conscience anormaux, ainsi que sur les importantes précautions à prendre dans la recherche électrophysiologique.

Mots-clés: Magnétoencéphalographie ; électrophysiologie ; LSD ; MEG; Connectivité interfréquence ; Wavelet ; Transformée Synchrosqueezing

Abstract

The past decade has seen a number of significant advances in mathematics, computational learning, and signal processing, which have yet to be deployed in neuroscience. In particular the assessment of connectivity in neural networks has much to gain from this work. Here we propose these tools be leveraged to partially bridge the considerable gap that still exists between large-scale connectomics research (largely centered around indirect measures of brain activity such as fMRI), and more direct, physiological measures of brain activity. Bridging this gap is especially important to the study of physiological properties associated with various normal and abnormal states of consciousness including Psychiatric conditions, sleep, anaesthesia or drug-induced states. Exemplary of such research, is recent work surrounding the induction of altered states of consciousness by non-selective serotonin agonists such as Psilocybin and LSD.

During the past five years, a rapid resurgence of research into the neurobiology of Psychedelic tryptamines has transpired, following a half-century hiatus. While these substances hold great potential to illuminate hitherto uninterrogated aspects of normal and abnormal brain function, the scope and unusual character of the changes they illicit pose serious challenges to researchers. Uncovering cogent and scalable methods for investigating such data is a matter of great importance if we are to leverage the unique window such atypical substances provide into central aspects of consciousness and abnormal brain function. In the present thesis, we summarize the current state of electrophysiological neuroimaging as it pertains to the study of Psychedelic tryptamines, and demonstrate a number of clear shortcomings in current electrophysiological research on Psychedelics. We also offer some modest methodological contributions to the field. The utility of these contributions is supported by some intriguing, albeit preliminary, empirical findings. In the first chapter, we present the history of neuroscientific research on LSD. LSD has been reported to induce peak shifts in power spectra, alongside decreases in peak amplitude. The fact that these effects are inter-related and most research so far has not sought to disambiguate them is uniformly overlooked in the literature, which we believe may lead to false interpretations.

Chapter Two discusses some of the plausible advantages as well as serious barriers to whole-brain connectivity research in MEG, proposing several strategies to overcome these

methodological limitations. These include cogent source imaging strategies, novel and recent developments in spectral decomposition, connectivity measures insensitive to volume conduction, and scalable implementations of well-established cross-frequency coupling metrics. We show that these techniques can be extended to a higher resolution cortical and subcortical grid than previously shown. We also discuss a lightweight implementation of non-parametric statistics suitable to such data. Chapter Three serves to demonstrate the efficacy of these procedures, showing empirical results from a whole-brain study of connectivity under LSD in MEG. The fourth and final chapter discusses these results, as well as necessary precautions and promising future directions for this kind of research. It proposes additional computational approaches that might extend the scope of such research and whole-brain electrophysiology more generally. Taken together, the methodological framework proposed in this work overcomes previous limitations endemic not only in Psychedelics research, but electrophysiological research broadly, and sheds new light on central mechanisms underlying these abnormal states of consciousness, as well as important precautions in electrophysiological research.

Key-words: Magnetoencephalography ; Electrophysiology ; LSD ; MEG ; Cross-frequency Coupling ; Wavelet ; Synchrosqueezing Transform

Table des matières

Liste des tableaux

Liste des figures

Liste des sigles et des abréviations

fMRI	*functional Magnetic Resonance Imaging*
LSD	*Lysergic Acid Diethylamide*
MEG	*Magnetoencephylography*
EEG	*Electroencephalography*
STFT	*Short-time Fourier Transform*
FFT	*Fast-Fourier Transform*
PSD	*Power Spectral Density*
CSD	*Cross Spectral Density*
5HT2AR	*Receptor for subtype of 5-Hydroxytryptamine 2 (Serotonin)*
WT	*Wavelet Transform*

PT	*Psychedelic Tryptamine*
GSR	*Global Signal Regression*
FC	*Functional Connectivity*
HZ	*Hertz, number of oscillations per second*
PAC	*Phase-Amplitude Coupling*
CFC	*Cross-frequency Coupling*
PLI	*Phase-lag Index*
OAC	*Orthogonalized Amplitude Correlation*
GFC	*Global Functional Connectivity*

Remerciements

This work would not have been possible without the support of Irina Rish, Ishan Walpola, Guillaume Dumas, Karim Jerbi, Celine Begin, Pierre Bellec, Bratislav Misic, Joerg Hipp, Suresh Muthukumaraswamy, Robin Carhart-Harris, Dominique Alexander, and Awa Mbodj. I thank Irina Rish for her ongoing interest and support, as well as many inspiring conversations. I also thank her for her role on this committee. I thank Suresh and Robin for sharing data with me, for initially encouraging this research and giving me the opportunity to work on the first LSD paper. I thank Dr. Hipp for many interesting conversations and for guiding this work in its early stages. I thank Dominique Alexander and Ishan Walpola for inspiring conversations related to this work and friendship. I thank Guillaume Dumas for agreeing to be on my committee, and for interesting conversation. Hoping there will be more to come. I thank Pierre Bellec for his role as co-supervisor. I thank Celine for having helped me through an unusual number of administrative crises. Above all I must thank Karim for his ongoing support, advice, and patience, and Awa for her love and support, for keeping me (relatively) sane and balanced through this work.

Introduction

Since the discovery of the electroencephalogram (EEG) in 1924 by Hans Berger, investigations into human electrophysiology have had as a central preoccupation the characteristic alterations of the electromagnetic frequency spectrum observed during well-defined divergent states of consciousness. Before the taxonomization of electrophysiological effects accompanying sleep and waking, two prominent discoveries were made that would form an indisputable cornerstone for research in electrophysiology, and the basis for unresolved questions extending into the present day. The first would be the presence of a single dominant oscillation, persistent in all mammalian brains during simple restful waking, aptly labeled alpha. The second would be a reliable attenuation of this rhythm during visual and sensory stimulation, known as "the Berger effect." Enduring at around 10 hz, the alpha rhythm drew the interest of a diverse cast of scientists– specialists and non- – eager to explain its function. Early cyberneticist and biological mathematician Norbert Wiener famously sought to explain alpha as a mean effect of multiple oscillatory dynamics, while more recent theory has conventionally either endorsed this idea indirectly, via Kuramoto-like dynamics of multiple oscillators, or posited alpha and its attenuation as a by-product of cortical synchronizations and desynchronizations with definite thalamic drivers (Lozano-Soldevilla, 2018; Liley & Muthukumaraswamy, 2020; Strogatz, 1994). Alpha has been explained in terms of sensory gating, proffered as a plausible "sampling rate" of sensation, implicated as critical rhythm in memory formation, and suggested to be a critical mediator in neural feedback processes involving various forms of cross-frequency-coupling (travelling waves), but its basic nature is still not well understood. (Klimensch, 1997; Palva & Palva, 2015; Samaha & Postle, 2015; Spaak et al 2014;Ronconi et al 2018; Haegens et al 2011; VanRullen & Koch, 2003; Alamia & Vanrullin, 2019; Bahramisharif, et al 2013; Pang et al 2020; Zhang et al 2018).

The current manuscript presents recent work in pharmacological MEG which illuminates hitherto unseen aspects of alpha activity under abnormal states of consciousness. It aims to highlight some of the relationships between alpha and such atypical forms of cognition as those elicited by serotonergic psychedelic drugs, while exploring the plausibility and shortcomings of previous research assessing the functional significance of these effects. Most importantly, it presents novel insights into the relationship between alpha and various indices of

interregional synchronization in MEG, while addressing extant methodological barriers and putative solutions to conducting electrophysiological analyses at a very large scale.

Chapitre 1

Historical and Scientific Context of Research

1.1. Historical Context

Lysergic acid diethylamide (LSD) is a non-selective serotonin-receptor agonist synthesized in 1938 and identified as psychoactive in 1943. During the 1950's, research into the consciousness-altering properties of LSD prompted a veritable sea-change in Psychiatry and electrophysiology. Thought to provide a window into abnormal cognition, research on LSD flourished for two decades until fears surrounding its growing popularity prompted a widespread moratorium on human research lasting through the first decade of the current century.

In the years spanning the discovery of LSD, its subsequent ban, and the eventual resurgence of psychedelic research, studies of it, and of related substances, have presented a muddled picture of the behavioral impact of LSD. In early research, LSD was found to either increase (Becker 1967; Blough, 1956, 1957a), decrease (Fuster, 1959; Key, 1961; Sharpe et al., 1967; Siegel, 1969) or have no effect (Berryman, 1962; Dykstra, 1973) on temporal discrimination in a range of psychophysical experiments. Studies also attested to significant alterations in absolute visual and auditory threshold with contradictory effects on reinforcement learning in a range of behavioral task (Dykstra, 1973). Due to often substantial divergences in dosing, paradigm, and the animals utilized in such research (decorticated vs intact cats , pigeons, monkeys and rats), such inconclusive findings are unsurprising. Nevertheless, studies from this era attest near-universally to at least two prominent effects of LSD: a substantial reduction in amplitude affecting all frequencies measurable by EEG–especially alpha– and an increase in peak frequency of the alpha rhythm (Shagrass, 1967).

Findings related to the neuropharmacological action of LSD have been more consistent, showing reliable increases in the tonic activity level of the optic tract and lateral geniculate body (Schwartz & Cheney, 1965), alterations in the recovery cycle of excitability in auditory and visual cells (Purpura, 1956; Davis et al 1975), and preferential influence on entorhinal and hippocampal cortices, (Adey et al, 1963). LSD in particular has been shown to exert its influence via a special affinity for the Serotonin binding 5-hydroxytryptamine(5-HT)

system shared by all tryptamine psychedelics (Berridge & Prince 1974), thus preferentially binding to regions mediating a range of cognitive and somatic processes, including the choroid plexus, frontoparietal cortices, motor, premotor and somatosensory areas, olfactory tubule, anterior cingulate gyrus, nucleus accumbens, caudate-putamen, claustrum, dentate gyrus, mammillary nuclei, and motor trigeminal nuclei (Nakada et al. 1984; McKenna et al 1989; Wong, 1987).

1.2. Contemporary Research

Following a resurgence of human research on psychedelics in the past decade, the effects of psychedelics on human brain activity have been interrogated using modern equipment with paradigms geared toward uncovering alterations in structural and functional connectivity. Several studies applying positron emission tomography (PET) to psychedelics have revealed increased cortical glucose metabolism (CMRglu) in 5HT2A-rich sites such as the frontomedial and frontolateral cortex, thalamus, anterior cingulum, and temporo-medial cortex, as well as thalamic, visual and sensorimotor areas (Vollenweider, 1997). These effects have been correlated with phenomenological effects such as visual hallucination and perceived "ego dissolution".

Less frequently acknowledged is the impact of LSD and related psychedelics on nonserotonergic binding sites. Some studies have emphasized a significant impact on the Dopamine D2 and D3 systems, with additional impacts on alpha-1 adrenergic 5HT1A system–namely the ventral (Nucleus Accumbens, Olfactory Tubule) and dorsal (Caudate-Putamen) striatum (Vollenweider,1999; Minuzzi, 2005; Seeman, 2005). The likelihood that this dopaminergic action is mediated by serotonergic effects is supported by several studies showing that the majority of psychedelic effects (though not all, as is sometimes maintained–see e.g. Carter, 2007) are blocked by the selective 5HT2A receptor antagonist Ketanserin (Vollenweider, 1998; Kraehenmann et al 2017;Preller et al. 2018; Quednow et al 2011).

Multimodal analyses employing structural assays alongside fMRI blood-oxygen level dependent (BOLD) signal reveal a range of supplementary effects of LSD on functional connectivity shown to be mediated in a nonlinear fashion by 5HT system binding. These findings beg the question of whether this effect is due to simple scaling of receptor densities, or something more mechanistically complex. Gustavo Deco (2018), has used mean-field modeling to identify the interactions characteristic of the relationship. In his work, PET-derived values of region specific serotonin concentration were integrated into a dynamic model of recurrent excitatory and inhibitory connections in the brain, as "neural gain" parameter quantifying the sensitivity of efferent firing rates within a neural population, to changes in input.A global parameter was incorporated to tune neural gain to simulate the proposed effect of LSD.

Comparing global time-averaged connectivity predicted by the model and the empirical results of BOLD connectivity under LSD, Deco found support for 5HT2AR-density scaling as a central mediator of LSD drug action.

Notable established changes in functional connectivity under psychedelic substances include decreased BOLD signal in various “hub-like” regions, including the thalamus, anterior and posterior cingulate and ventromedial prefrontal cortex, as well as sensory regions, accompanied by substantially altered connectivity between them. Most prominently, LSD is seen to induce increases in global functional connectivity between these regions and the rest of the brain, facilitating a broadened repertoire of possible connectivity "motifs". In similar fashion, Carhart-Harris et al. (2016) observed decreases in connectivity within typically segregated brain networks, alongside increases in between-network connectivity in all but one network pair (visual-frontoparietal). This latter finding implicates several 5HT2 rich regions (frontal, parietal, and inferior temporal cortices, as well as in the bilateral thalamus) as emergent hubs facilitating increased global connectivity under LSD, with particularly robust connections to auditory, sensorimotor, and visual networks (Muller et al 2018). Finally, while decreases in network segregation were not associated with more specific behavioral measures such as ego-dissolution, increases in global connectivity, and especially those between aforementioned sensory cortices and bilateral angular gyrus and insula-region did correlate strongly with both perceived intensity of the experience and ego-dissolution (Carhart-Harris,2012; Carhart-Harris, 2016; Tagliazucchi,2016).

The general effect of increased functional network integration under LSD is robust. Nevertheless, inconsistencies have emerged in the precise location of these effects. For example, Preller et al (2018) have demonstrated that while results of Tagliazucchi’s 2016 fMRI study, showing increased connectivity in associative cortices (especially prefrontal and angular gyrus, and cingulate areas), were easily reproduced, these effects were eliminated by global signal removal, resulting in the contradictory finding of global hypoconnectivity under LSD in thalamic and associative regions, and hyperconnectivity in sensory cortices. While the authors of this study concede that this global signal regression (GSR) may be seen to remove legitimate neural activity alongside plausible artifacts, and controversy surrounding the use of GSR persists (Murphy & Fox, 2017), this finding underlines the sensitivity of observed functional connectivity to modality and data preparation: a point which will be of critical importance to the research presented later in this manuscript.

In a somewhat more nuanced analysis, Luppi et al (2020) have shown (without GSR) that global BOLD connectivity under LSD is non uniform over time, and is instead comprised of two orthogonal substates: one consisting of higher levels of global network segregation– and the other of higher network integration, under which state small-worldness is seen to mediate ego-dissolution. Bridging Preller’s and Tagliazucchi’s contradictory results, Luppi shows global dynamic functional connectivity to be decreased in associative cortices–especially

fronto-medial and anterior cingulate cortices– only during states of high segregation. This effect is not observed in time-averaged analyses. Increases in thalamic connectivity (with orbitofrontal-insular, temporoparietal and bilateral amygdala sources) were also observed by Luppi, independent of integration level.

A principal finding of Luppi's study was that during the more transient, less temporally dominant high-segregation state, LSD was seen to induce "the opposite effect to anaesthesia, allowing FC to diverge more freely from anatomical constraints." Whereas high similarity between functional and structural connectivity (as measured by Hamming distance) was observed in high integration states, high segregation states under LSD were marked by substantial attenuation of the similarity between functional and structural connections. This study is of interest for the reason that it highlights the dynamic character of LSD's influences on connectivity, and the dynamic character of (generally mediating) 5HT2A-dense "hubs." It also complicates a somewhat simplistic picture proffered by time-averaged BOLD and global mean-field approaches.

The effects observed in dynamic BOLD analyses prove that LSD action is complex in ways that cannot be untangled without scrutinizing the influence of time. The variable nature of these effects in time is further supported by recent studies suggesting that psychedelics tend to enhance the entropy of neural signals (Varley, 2020), as well as the repertoire of connectivity motifs (Petri,2014; Tagliazucchi et al., 2014), with connectome harmonics operating nearer to criticality (Atasoy, 2017). This finding facilitates an understanding of the seemingly contradictory effects outlined by Luppi's study, as criticality can be understood to correspond to a phase transition between a sub-critical state–a comparatively inflexible, highly ordered and displays low entropy (high segregation)–and a super-critical state–highly entropic, flexible, and disorganized (low segregation).

A version of Deco's mean-field modeling approach was recently applied to Psilocybin incorporating much more detailed mathematical descriptions of temporal dynamics. Kringelbach et al. (2020) paired dynamical equations for synaptic/neuronal activity and neurotransmitter diffusion via the same receptor maps used in Deco (2018). By accounting for synaptic dynamics, directedness of anatomical pathways and the excitation of afferent projections from serotonin producing regions, the model was able to accurately predict empirical coupling (state probability, lifetime, and transition probability) and identify regionally specific modulation of global dynamics based on aforementioned site-specific gain parameterizations and the firing rate of the raphe nucleus (van der Meer, 2018). Madsen et al (2019) has also shown receptor occupancy to be correlated with dynamic effects of LSD using mean-field models. In this vein, but more illustrative of site-specific "hubness" is Herzog et al's (2020) study, which recently applied dynamic mean-field modelling to LSD, showing regionally specific impact on local entropy with strong correspondences to connectivity-strength

an 5HT2AR density. Such mean-field modelling might be usefully applied to the identification of specific mechanisms responsible for observed electrophysiological changes as well.

1.3. Electrophysiological Research

Despite relatively conclusive results on the location and character of functional connectivity changes under psychedelics as measured by BOLD, the research outlined above remains a limited basis for mechanistic explanations of LSD action. One important drawback of this work is its tenuous connection with actual neuronal activity. While PET and fMRI no doubt possess the advantage of high spatial resolution as measures of neural energy consumption, the time-scale on which they operate is many orders of magnitude removed from that of local field activity. In order to properly account for the precise nature of rhythmic activity on inter-regional coupling under LSD and other tryptamine psychedelics, comprehensive understanding of the relationship between alterations observed in electrophysiological and BOLD data is required.

As mentioned previously, historical research on LSD has identified two predominant effects on human electrophysiology: widespread decreases in oscillatory amplitude, particularly in alpha, and a robust increase in peak alpha frequency. These effects have been replicated with an array of 5-HT2A agonists using local-field potential recordings in rodent brains, as well as human EEG (Horovitz et al, 1965; Abraham et al 1996;Celada et al. 2008; Wood et al 2012). Contrary to older research, which was limited in the range of frequencies detectable by EEG, a number of modern EEG-based studies show lower spectrum oscillatory amplitude decreases to be accompanied by significant increases in high-frequency (gamma) activity under psychedelics (Stuckey et al 2005; Gonzalez et al, 2020). Others have shown reliable increases in high-gamma activity via intracranial EEG in rodents in psychedelics (Páleníček et al, 2013; Goda et al. 2013; Gonzalez et al 2020).

In one of the first robust human studies, Muthukumaraswamy et al (2013) investigated alterations in oscillatory activity under Psilocybin using MEG. The study showed broadband decreases in oscillatory power distributed over a number of functional networks. These broadband decreases in power are believed to be caused by irregular excitation of layer 5 pyramidal neurons– a hypothesis which predicts decreases extending into gamma and high-gamma domain, and supported by dynamic causal modeling. This desynchronization explanation has been a dominant paradigm for interpreting psychedelic effects in the majority of subsequent electrophysiological studies (Barnett, 2019; Carhart-Harris, 2016;Carhart-Harris, 2019; Liley and Muthukumaraswamy, 2018; Pallavicini, et al. 2019; Tagliazucchi, et al . 2016). Exemplary of theoretical interpretations of this effect, the first multimodal study of LSD summarizes the alpha effect as follows:

> «*Cortical alpha has been hypothesized to serve a general inhibitory function, filtering out 'stimulus-irrelevant' information. Thus, reduced alpha power could have dis-inhibitory consequences, facilitating the release of anarchic patterns of excitation that manifest spontaneously and experientially as visual hallucinations (Carhart-Harris et al, 2016).* »

The recently-proposed REBUS ("relaxed beliefs under psychedelics") hypothesis, which aims to establish the principal psychedelic effect on neural activity as a kind of reversal of top-down and bottom-up processing (within a predictive coding framework), similarly claims:

> «*It is well known that the brain's resting power spectrum exhibits stark nonuniformities in its oscillatory components, in the sense that certain rhythms are especially pronounced. This seems to be particularly the case when recording population-level activity in the cortex. Perhaps the most conspicuous example of a predominant rhythm is the α rhythm or Berger wave of about 10 Hz, which shows a striking prominence, especially, but by no means exclusively, during eyes-closed waking rest. The α rhythm has been associated with a range of functions, including top-down inhibition (Klimesch et al., 2007). Evidence has been accumulating, however, that α also plays a more specific role in conferring top-down expectations about perceptual stimuli (Mayer et al., 2016) that effectively silence more granular information processed by lower-level aspects of the system. The α power is known to correlate positively with DMN activity (Mantini et al., 2007), as does β (Mantini et al., 2007). Like alpha, the β rhythm has also been associated with a top-down function, albeit within the motor system (Fries, 2015).* »

The authors add,

> «*the α rhythm is known to be especially highly expressed in humans relative to other animals, and especially so during maturity, with a peak at about 20 years of age (Basar and Guntekin, 2009), which, intriguingly, is approximately when the complexity of cognition has been found to be maximal (Gauvrit et al., 2017). Although open to critique, a curious cross-cultural electroencephalogram (EEG) study sampling eyes-closed brain activity in more than 400 individuals has reported that α is most pronounced in the most technologically advanced and developed cultures (Parameshwaran and Thiagarajan, 2017). (Carhart-Harris & Friston, 2020)* »

It is well established that some of the effects of psychedelics on functional network segregation observed via fMRI are possibly mediated by decreases in cortical inhibition (Müller et al 2017). However, the description of alpha as a simple marker of "cortical inhibition" is dubious. Apart from the somewhat problematic dual claim that large alpha expression is an index of both entropic/complex thinking and of "fixed beliefs," the articles cited on alpha (and beta) are highly selective and misleading. Pointing on the one hand to decreases of alpha in the PCC as an indication of alpha's BOLD-like status in electrophysiology, and on

the other hand, alpha's presumed anticorrelation to BOLD resting-state activity (Carhart-Harris et al, 2016), the authors infer spatially distributed meaning from site specific effects —which are moreover seen to be distributed across the frequency spectrum.

Alpha is not simply associated with resting state activity, but is host to a range of effects whose precise relationship to BOLD is anything but clear (for a robust overview, see Palva & Palva, 2007). It has, for example, been shown to be functionally anticorrelated with beta and gamma, both of which hold parallel significance for the authors' interpretation as they are presented as systematically reduced under psychedelics (Pang & Robinson, 2018; Sadaghiani & Kleinschmidt, 2016; Carhart-Harris, et al. 2016; Muthukumaraswamy, 2013; Barnett et al 2020) . This latter claim is not universally supported by the research (Timmerman et al 2017; Goda et al. 2013; Gonzalez et al 2020).

Better evidence for their central claim –that psychedelics facilitate increased influence of sensory and environmental stimuli, and a decreased role of "top-down" priors for cognition– comes from the host of studies, both historical and current, citing alterations in perceptual discrimination and learning across a range of behavioral assays in both animal and human subjects. Timmerman et al. (2018) have shown alterations auditory discrimination accompanied by change in directional connectivity, and neural sensitivity to novel vs familiar stimuli, in a mismatch negativity paradigm. Another compelling study is that of Alamia et al (2020; See also Timmerman, 2019), which observed a change in direction of travelling alpha waves in sensor-level DMT.

In general the established role of alpha and other oscillatory activity in mediating processes of sensory gating and attention provides a stronger foothold for theorizing indices of psychedelic action in human electrophysiology. A substantial literature on alterations in oscillatory sensory gating as important predictors of positive and negative schizophrenia symptoms are suggestive here (Keihl et al, 2015; Thoma et al 2005; Fodor et al 2020).

In addition to changes in oscillatory power, both Psilocybin and LSD have been shown to induce increased signal diversity (Schartner et al, 2017), and to prompt visible and systematic shifts in peak oscillatory alpha frequency, accompanied by changes in aperiodic spectrum (Lilly et al , 2018). Given previous literature attesting to a plausible functional significance of peak oscillatory frequency (especially in alpha), (Posthuma et al 2001; Clark et al, 2004;Mierau et al 2017; Lozano-Soldevilla, 2018), the impact on oscillatory peak shift is a matter which has been insufficiently investigated. Furthermore, alterations in peak oscillatory frequency introduce a confound to the direct comparison of either band-wise, or frequency-specific oscillatory effects (Liley, 2018;Nest, 2018). While (amplitude-based) connectivity results have recently been presented for LSD and Psilocybin, these were computed using band-wise power, and fail to control for changes in peak oscillatory frequency (Pallavicini, et al. 2019;Barnett et al, 2020; see also Anzolin et al 2019, which highlights the influence of source-estimation methods on directed coupling in MEG).

1.3.1. Gaps in Research and Objective of Current Study

Although alpha is purported to mediate the observed effects of LSD, and is believed to underlie several of the observed changes seen in fMRI connectivity, it is as yet unclear what impact the shift in peak alpha frequency, and associated broadband changes in the periodic and nonperiodic frequency spectrum might have on observed connectivity effects across the brain. In particular, these frequency shifts likely have confounding effects on the results derived from analyses of power and connectivity effects in MEG, prompting us to derive erroneous conclusions from spurious relationships. Furthermore, the sources associated with these cross-spectral effects, and their impact on whole brain relationships is not currently known. In light of the known role of alpha in mediating not only "top-down" but also "bottom-up" cognition via travelling waves, and sensory gating, the investigation of these effects warrants further consideration.

In order to better illuminate the precise mechanisms of action in LSD induced electrophysiological changes, and to better ground the relationship between BOLD-based connectivity and electrophysiological effects, the present study will apply three connectivity measures corresponding to three plausible means of neuronal signalling and synchronization: one phase-based measure, one measure of amplitude correlation, and one measure of interregional phase-amplitude coupling (PAC). This study will also attempt to localize and better identify the precise character of observed frequency shifts and power changes.

Chapitre 2

Methodological Challenges

The previous chapter closed with a discussion of the special methodological challenges presented by pharmacological-MEG and especially LSD. Before presenting our own study methodology, it is important to discuss some of the more general limitations inherent in the utilization of MEG as a measure of source-level brain connectivity. These have no doubt played a role in the hitherto limited scope and largely hypothesis- (as opposed to data-) driven character of whole-brain electrophysiological research with MEG.

In general, barriers to large-scale, data-driven MEG connectivity analyses fall into three categories:

(1) Those associated with the scale of data resolved into constituent time-frequency characteristics

(2) Those associated with lowered resolution of temporal, frequency, and spatial characteristics caused by intermediary computational steps such as time-frequency transformation and source-projection

(3) Those associated with our statistical and/or predictive models and the identification of main effects due to extreme high-dimensionality (and tensor-structure) of data

These issues emerge alongside the significantly limited spatial resolution and signal-noise ratio (SNR) of scalp or sensor level electrophysiological recordings relative to fMRI, as well as their particular sensitivity to muscle and other kinds of artifacts. Apart from the aspects most immediately relevant to our own data (namely increased presence of muscular activity assumed to be induced by the consumption of LSD and other serotonergic tryptamines), we will exclude this rather high-level topic (on which there are several high-quality treatments in the literature; see for example Sekihara, 2017; Hedrich, 2005) from the present discussion. Nevertheless, great consideration was taken in our selection of source-imaging metric (to be discussed in the following section).

2.1. Challenges Associated with the Scale of Data

Owing to the considerable size of data resolved across both time and frequency, it is infeasible with currently-available hardware to perform resting-state analyses on MEG data at spatial resolutions comparable to standard fMRI connectomics. It is standard instead to identify a domain of interest in the temporal, spatial, and frequency dimensions. It is also common (and valid) to report results from sensor-level MEG, and in spatially projected data, it is typical to either bin data into anatomically significant ROIs, or to select regions and frequencies of interest (Hawellek et al. 2013). Studies applying high spatial resolution MEG (>1000 voxels) resting state data, at more than 7 or so frequency bins are few. Due to the massive number of empirical frequencies resolved under the (largely untenable) assumption of stationarity–on the order of $(fs \times ns)/2$ where fs = "sampling rate" and ns = "length of recording in seconds"– reducing the frequency domain to binned frequencies of interest, associated with historically and physiologically relevant oscillations such as alpha, beta, gamma, and delta, is standard practice. As we have seen in the above discussion, however, systematic (and often subtle) alterations in the structure of the frequency spectrum across pharmacological (Muthukumaraswamy & Lily, 2018), as well as psychiatric(Nikulin et al, 2012; Uhlhass & Singer, 2010; Hoptman et al. 2010) and cognitive conditions (Posthuma et al 2001; Clark et al, 2004;Mierau et al 2017) are likely more fundamental an index of the mechanisms underlying these conditions than has been previously realized (Muthukumaraswamy, 2014). Accordingly, and for reasons to be further elaborated below, it can be advisable to consider a range of frequencies covering the full spectrum of oscillatory effects (Hipp et al 2012; Hawallek et al 2013).

While a number of valid approaches have been successfully employed for deriving arbitrarily resolved frequency estimates of rhythmic activity in time (e.g. Short Time Fourier and Hilbert Transforms), the Wavelet is undoubtedly the most recent, and theoretically robust among them. In addition to providing an empirically resolved analytic signal, parametrically balancing the standard deviation of filters in both temporal and frequency domain, wavelets have the advantage of being fully invertible, making them indispensable to a host of research applications ranging from seismology to the detection of gravitational waves–in addition to their numerous practical applications in sparse representation and digital compression (Klimenko, et al 2002; Picco et al 2019; Tsang et al 2020).

Though the computational barriers traditionally associated with managing data objects at the scale necessary for data-driven source-level connectivity in MEG persist, several developments have made such analyses feasible. Most importantly architecture supporting high-memory hardware has become exponentially cheaper and more accessible in recent decades. Secondly, the development of software such as CUDA, which support extremely fast matrix computation by leveraging GPU architecture, and the increased availability of high memory

GPU chips, reduce compute time for nearly all aspects of a MEG connectivity pipeline–from projections to source level (matrix multiplication of n dipoles × n sensor imaging kernel and data matrix of size n sensors × n samples matrix), convolution (or fourier domain multiplication)of the wavelet kernel, inner products of the phase and amplitude components of analytic signal needed for cross-frequency coupling, to computation of phase and amplitude based synchronization across all pairs of vertices (and at each frequency bin). Finally, a great number of open-source software frameworks have emerged in recent years which facilitate the use of high-power-computation (HPC) clusters, management of resources, and optimization of algorithms, with high-level coding paradigms like python.

Examples of such libraries are Slurm, Apache Arrow, Numba, PyCuda, PyPERL Dask, and Ray. Ray, in particular, allows one to leverage access to multiple gpus and cpu nodes, while preserving in memory any number of data objects via Apache Arrow's plasma object store. This makes possible rapid asynchronous computation without multiplication of data objects in memory entailed by standard asynchronous and threaded data processing frameworks (e.g. multiprocessing in python, or the built-in Mpool and Task objects of Matlab and Julia respectively). Additionally, numba, and PyPerl allow the rapid development of cached and python-free just-in-time implementations of functions resulting in exponential speed gains, while PyCuda, Cupy and Dask allow one to leverage the advantages of gpu-based matrix computations with simple numpy code. These softwares and libraries were indispensible for the analyses described here . By means of them, relatively lighter weight and asynchronous implementations of morse wavelets, various connectivity algorithms and jit-ified statistical functions were developed to make manageable the heavy computational overhead created by such large data objects.

2.2. Challenges Associated with Resolution in Source-Level MEG

2.2.1. Source Estimation and Synchronization

Source-level MEG suffers from limited spatial resolution compared with fMRI for reasons related to the intractable nature of its inverse problem. While researchers have proposed empirical fixes to the problem of no ground-truth, including incorporation of bayesian priors (Wipf et al 2010) and SNR estimation derived from other modalities (Hipp & Siegel, 2015), these are often unwieldy and/or require additional data that are not always readily available. Until fairly recently, it has not been clear that MEG source-estimation algorithms were capable of detecting deep and subcortical sources, yet consensus has emerged supporting the reliability of deep source estimation (Attal et al, 2013; Bénar et al 2021; Piastra et al 2021; Recasens et al 2018). Source projection algorithms have improved considerably in quality

over recent years. In particular, exact low resolution brain electromagnetic tomography (eLORETA; Pacual-Marqui et al, 2007), the first 3D, discrete, distributed, linear solution to the inverse problem of EEG/MEG with zero localization error, shows significant benefits relative to other source estimation techniques (LCMV Beamformer, MNE and DSPM; Halder et al 2019; Mahjoory et al 2017; Anzolin et al 2019). By minimizing the second spatial derivative (surface Laplacian), eLORETA has been shown to yield reliable source estimations robust to SNR and with low occurrence of false-positives and superior performance in deep brain sources, and is thus an ideal conservative source model for exploratory analyses (Halder et al 2019).

Still, these estimations have limited degrees of freedom, and are seen to result in non-negligible volume conduction, with consequences for both spectral decomposition and connectivity analyses. Because electrophysiological signals are measured instantaneously at different sensors, their source-level projections reflecting multiple distinct sensors contain spurious identical phase components, despite it being known that distinct neural populations contain variable phase relations. To ameliorate these problems we apply the SNR regularization derived from Wens et al. (2015) in our source estimation procedure.

$$\kappa = \frac{\mathrm{tr}\left(C_{\varepsilon}^{-1} L L^{\mathrm{T}}\right)}{\mathrm{tr}\left(C_{\varepsilon}^{-1} C_{\mu}\right) - M}$$

As a control for field spread, we apply estimations of phase and amplitude-based coupling insensitive to volume conduction–namely the Orthogonalized Amplitude Correlation(OAC) proposed by Hipp et al (2012), and a weighted Phase-lag Index (PLI) proposed by Vinck et al (2011). OAC removes zero-phase components from each pair of source signals before computing a linear correlation of amplitude, to ensure power correlations are not affected by spurious field spread.Though these measures can not entirely ensure zero false-positives, and are likewise known to impact the separability of phase and amplitude-based coupling effects–see, for example, the note of caution presented by Palva et al (2018), also Wens, et al (2015) – previous studies have demonstrated their considerable efficacy in illuminating true distal coupling compared with classic methods such as simple amplitude correlation and phase coherence.

OAC achieves this by taking the orthogonal part of all pairwise signals before computing correlations. Specifically the complex signal $Y(t,f)$ orthogonalized to the complex signal $X(t,f)$ is defined:

$$Y_{\perp X}(t,f) = \mathrm{imag}\left(Y(t,f)\frac{X(t,f)^*}{|X(t,f)|}\right)$$

Similarly, PLI estimates near but non-zero phase relations between signals, under the assumption that most zero-phase coherence is likely due to field spread. If we are to take $I(X)$ and $R(X)$ as the imaginary and the real component of the cross-spectrum, respectively,

then EX = 0, when all sources are uncorrelated. Due to volume-conduction, however the inequality $E(R(X)) \neq 0$, indexes a spurious non-zero phase locking value and coherence (Nolte et al., 2004). Thus Imaginary coherence, defined as $I(C)$, provides a measure of phase-synchronization.The sign of the Imaginary coherence, $\text{sgn}(\Im C)$, indicates whether signals from the first sensor tend to phase lead or lag signals from the second sensor, and the strength of phase-synchronization can be indexed by the absolute of $|IC|$.

Because IC is influenced by the phase of coherency, it has the shortcoming of high sensitivity to noise. Hence Stam et al (2007) introduce PLI, defined as: $\Psi \equiv |E\{\text{sgn}(\Im\{X\})\}|$

Due to biases inherent in PLI, a debiased version is introduced as:

$$\Phi \equiv \frac{|E\{\Im\{X\}\}|}{E\{|\jmath\{X\}|\}} = \frac{|E\{|\mathcal{I}\{X\}|\,\text{sgn}(\Im\{X\})\}|}{E\{|\mathcal{I}\{X\}|\}}$$

WPLI is less sensitive to noise than PLI and is shown to have a more reliable relationship with true phase consistency, even under conditions of high SNR(Vinck et al, 2011).

2.2.2. Frequency Estimation

A notable limitation of electrophysiological analyses (at source-level or otherwise) is the tradeoff between frequency and time resolution inherent in all forms of spectral decomposition. Fourier transform, for example, gives perfect resolution in the frequency domain while collapsing the temporal dimension. As alluded above, wavelets overcome this discrepancy somewhat by balancing temporal and frequency domain resolution. Morse wavelets (Lilly & Olhede, 2012), defined in the frequency domain as

$$\Psi_{\beta,\gamma}(\omega) = \int_{-\infty}^{\infty} \psi_{\beta,\gamma}(t) e^{-i\omega t} dt = U(\omega) a_{\beta,\gamma} \omega^{\beta} e^{-\omega^{\gamma}}$$

are favorable due to their exact analyticity, and their ability to reproduce all known forms of analytic wavelet by means of only a time-frequency tradeoff parameter gamma, and a skewness parameter beta, yield a continuous time analytic signal where time-frequency tradeoff can be tuned to the exact demands of the analysis in question. They also provide a simple equation for computing the Heisenberg area–that is, the domain in frequency and time space where edge effects and aliasing are assumed to be negligible, and where time-frequency estimates are therefore known to be valid–from wavelet parameters.

Such a trade-off nevertheless results in unavoidable smearing which can obscure meaningful effects when said effects are sufficiently near in either the time or frequency domain. Because this study is interested in delineating effects of sometimes adjacent frequency bins (10 vs 12 hz peak in alpha), the ability to clearly identify effects in one or the other frequency bin would be an obviously attractive feature of our pipeline. Fortunately such a method has emerged in the past decade. The Synchrosqueezing Transform (SST; Daubechies, et al. 2011) emerged as part of an attempt to ground Empirical Mode Decomposition, and the

Hilbert-Huang Transform theoretically (Huang & Wu, 2008). While there have been several similar attempts to model a nonstationary signal as a superposition of oscillatory modes

$$x(t) = A_0(t) + \sum_{k=1}^{K} A_k(t) \cos\left(2\pi\phi_k(t)\right)$$

– typically referred to in the literature as adaptive harmonic models (AHM)–SST is a theoretically valid method ideally suited to wavelet analysis. The method is reliable, invertible and extremely computationally efficient. It works by reassigning scale according to instantaneous frequencies in order to sharpen the time-frequency representation of a signal, allowing one to partially overcome limitations on resolution imposed by Heisenberg uncertainty. SST, which provides an alternative to the EMD method and its variants such as the ensemble EMD (EEMD), carries many of the advantages of EEMD and other AHMs for frequency-based analyses, while overcoming some limitations of the EMD and EEMD schemes such as mode-mixing and the presence of negative instantaneous frequencies (Wu & Daubechies, 2011, Meignen et al, 2012; Auger et al 2013).

In addition to its ability to independently resolve nearby frequencies, our use of SST was motivated in part by emerging problematization of common practices in the estimation of phase-amplitude coupling using traditional parametric spectral methods (Giehl et al. 2021; Yeh et al. 2016). Such approaches have been called into question on the basis of the plausible spurious detection of PAC due to detection of signal higher-harmonic power arising from non-sinusoidal brain-oscillatory activity. The more the detected signal deviates from a sinusoidal function, the larger the coefficients of higher harmonics. As a result AHM based approaches to PAC have been proposed. In particular, Hilbert transformed EEMD has become a popular means of PAC estimation in the past few years (Pittman-Polletta et al 2014; Tsai et al, 2019; Yeh & Shi, 2018). While the use of analytic wavelets rather than parameterized band-based Hilbert or Fourier estimation already controls for some known sources of spurious PAC (Jensen, et al 2016; Sotero, 2015a, 2015b; Dellevale 2020; Kovach et al, 2018; Munia et al 2019), SST is well suited to the assumption of non-stationary and non-sinusoidality in signals. To our knowledge we are the first to use SST in an Adaptive decomposition-based implementation of PAC.

A final and somewhat auxiliary concern is the independent resolution of oscillatory and aperiodic frequency spectra. While electrophysiological activity has long been acknowledged to be comprised of both oscillatory components and aperiodic components, it is as yet unknown what influence these disparate rhythmic and arrhythmic oscillatory features have on spatial and connectivity metrics–including PAC (He et al 2010). Only recently have tools emerged for separately estimating the oscillatory and aperiodic components of power spectra. Notably the Fitting Oscillations and One-over F (FOOOF) method achieves this by fitting a linear model to 1/f frequency spectrum as well as divergences from this spectrum (Donoghue

et al 2020). It is a parametric method which can detect a range of oscillations within a predefined frequency range in a signal. As a nonparametric alternative, IRASA has been proposed (Wen & Liu, 2016). This method works by taking a signal power spectrum density(PSD) as well as the median of PSDs of the geometric mean of the same signal resampled at several non-integer factors and their inverse. Since this can be said to provide a reliable estimation cross spectral aperiodic power, the aperiodic PSD is then subtracted from the original PSD to yield oscillatory power at all estimated frequencies. Still the IRASA method can yield only estimates of stationary oscillatory and aperiodic activity respectively. Due to the nonparametric nature of the IRASA algorithm and the fine-grained frequency resolution of synchrosqueezed morse wavelets, we propose WIRASA–a wavelet-based estimation of aperiodic and rhythmic power which can be resolved in time with superior resolution to trial-based IRASA, with slight speed improvements. We ensure unbiased wavelet estimation of PSD following the procedure outlined in Liu et al (2007), and increase the frequency resolution of the morse wavelet considerably to ensure oscillatory frequencies are correctly resolved. Theoretically this can allow dynamic comparison of oscillatory and aperiodic source coupling, though such an approach is not pursued in the present document.

2.3. Statistical Challenges

A final important challenge to address is that of statistics. The large dimensionality, and tensor-structure of source-level, full spectral MEG connectivity data lends itself to a host of problems. Firstly, parametric statistics are ill-suited to such data since SNR and variability cannot be assumed to follow a Gaussian or uniform distribution across all dimensions of the data. Accordingly, permutation and rank-based statistics are strongly recommended. This lends itself to computational challenges. Specifically in addition to the pragmatic challenge of running preliminary analyses for n subjects $\times$ n observations $\times$ n conditions, one must have access to sufficiently high-memory computational resources to fit at least one instance of the data structure in question, for purposes of multiple comparison and/or bootstrapping. Individual permutations, on the other hand (which must be run a minimum of 1000 times, and must represent only one data dimension $\times$ n subjects $\times$ n observations $\times$ n conditions at a time) can be performed using mmap with only slight damage to performance. In general the tradeoff between memory and computation time is a persistent challenge that proves unavoidable in these kinds of analyses.

An additional challenge is the inherent complexity of these analyses and the necessity of selecting regions or frequencies of interest (ROI, FOI) for purposes of vulgarization/reporting. This introduces additional branches of analysis as well as statistical biases that must be

controlled. As an efficient means of managing such problems , we use a rank-based permutational statistic procedure based on Hawallek et al (2013). First we count significant alterations between conditions as identified by our base statistic (Wilcoxon rank-sum $p<0.05$). We do so across each data dimension for each direction independently. We count the number of significant alterations along each dimension of each direction of the data tensor independently (counts of significant connections per frequency are done independently of counts of significant connectivity by source and so on). We then swap condition labels for all subjects and re-run our base statistic at all tensor dimensions at least 1000 times. In order to control for baseline distribution across all data dimensions of the tensor, we create ranks for each data dimension across all permutations. For multiple comparisons we take the max rank of each of the n permutations and compare each data dimension value to the permutation value associated with maximal rank for that data dimension. Once we have chosen frequencies and sources of interest, we follow a more conventional procedure: comparing values of our base statistic to max permutation values (by rank) over all permutations for all data dimensions within and outside of the selected frequency. This controls for biases introduced by ROI selection.

One novel alternative to such statistics –when sufficiently high-memory computational resources are not available and/or avoiding the complexities of manual ROI and FOI selection is a concern–is to use higher order variants of multivariate models such as Partial Least Squares (PLS). While > 1000 permutations are still required, the requirement of ROI selection and representation of full data tensor is avoided. Rather than yielding maps of significance for each individual data-point (at n sources $\times$ n sources $\times$ n frequencies $\times$ n frequencies for PAC, as an example), methods like Higher-Order PLS (Zhao et al, 2012) provide loading vectors for each dimension of the data, offering a reliable and statistically meaningful summary of the main effects along each direction of the data tensor(without individual dependencies on other data directions, as in conventional PLS). We have presented results of a Higher-Order PLS implementation in Nest (2019). Though complementary to the current work, results from this study did not make use of inter-regional, but local PAC, nor did it apply SST, or the same imaging kernel (eLORETA, 2046 vertices). It is therefore considered preliminary, and for this reason, omitted from the present manuscript.

Chapitre 3

Experiment

The present chapter comprises the experimental portion of this manuscript, showcasing many of the methods described above. Discussion of these findings will be included in the chapter that follows.

3.1. Outline of Methodology for the Current Study

3.1.1. Experimental Paradigm

20 subjects were selected. Using planar gradiometer-configured MEG, subjects were scanned for 2 x 5 minute runs in Closed-eye, Open-eye, Video and Music conditions under both LSD and Placebo. Six subjects' data were omitted due to extensive artifacts (11 males, three females; mean age 32 $\pm$ 8.3). For the purposes of these analyses video and music conditions were excluded.

3.1.2. Data Treatment

Data were cleaned for artifacts using ICA and visual inspection. Subject MRI's were used for individual source projection using eLORETA with 2046 evenly spaced vertices (2.5mm) x 3 dipoles. Source kernels were projected onto a default MNI brain. For all subsequent analyses, data were transformed using Morse wavelets between 0.6 and 152 hz, at 5 voices-per-octave resolution, with parameters gamma=3, and beta=60. These parameters ensure an ideal trade-off between time and frequency resolution (Lilly & Olhede 2012). For source-level analyses, data were wavelet transformed. For each cortical source, and at each frequency resolved, three filters were reduced to a single the dominant dipole orientation. To achieve this kernels were weighted with the first eigenvectors' elements of the frequency transformed wavelet coefficient at each source location. Complex source signals were then derived by

multiplying the complex valued wavelet coefficients of sensor matrix by the reduced imaging kernel. Subcortical dipoles were treated as independent signals and averaged following computation of connectivity metrics.

3.1.3. Comparison of Power

Power was estimated across frequency using the above wavelet transform. As an unbiased estimate of PSD from wavelets, wavelet coefficients were squared and divided by scale for each frequency (Liu et al, 2017). For separate estimation of oscillatory and aperiodic power, the WIRASA method outlined in the previous chapter was applied alongside standard IRASA and FOOOF. For representation of standardized data, individual power estimates of the wavelet-derived power spectra were simply subtracted from mean. This value was then divided by the standard deviation of power estimates.

3.1.4. Connectivity Metrics

Connectivity metrics included one phase-based and one power-based method, both insensitive to volume conduction. For amplitude-based coupling Orthogonalized Amplitude Correlation (OAC; Hipp et al, 2012) was applied. For details, refer to the previous chapter. For phase-based coupling, weighted Phase-Lag-Index was used(Stam et al. 2007; Vinck et al 2012). Details for this method are likewise provided in the above chapter. Both PLI and OAC were computed at each of the 49 frequencies resolved by wavelet decomposition, and for each pair of source-level signals (2046 x 2046). For all connectivity metrics, wavelet coefficients were first decomposed using the Synchrosqueezing transform (SST) described above. Our implementation of SST is based on Jiang & Suter (2017).

3.1.5. Phase-Amplitude Coupling

PAC estimates were computed at all pairs of vertices for each phase x amplitude bin (2046 x 2046 x 49 x 49). Norm-direct PAC was chosen for the reason that it is fast and reliable, while being insensitive to cross-conditional variations in amplitude (Ozkhurt, 2012). Only bins where amplitude was greater than 2x the frequency of paired phase were considered for statistical analysis .

3.1.6. Statistics

All statistical analyses were computed using Wilcoxon rank-sum ($p<0.05$) as a base statistic. For each connectivity metric, initial statistical comparison was performed at each data dimension. Conditional labels were then randomly reassigned 5000 times for all dimensions of data to estimate null distribution at each data dimension. Null values of the base statistic

were then ranked along each data dimension; conditional statistics were compared to max rank for each permutation to derive p-values controlling for multiple comparisons.

Selection of frequency bins of interest was conducted by comparing counts of all significant effects (2046 × 2046 for PAC; (2046 × 2046)/ 2 for OAC and PLI) across all dimensions of data and comparing these to maximum ranking values for each permutation.

3.2. Experimental Results

3.2.1. Alterations in Cross-spectral Power under LSD

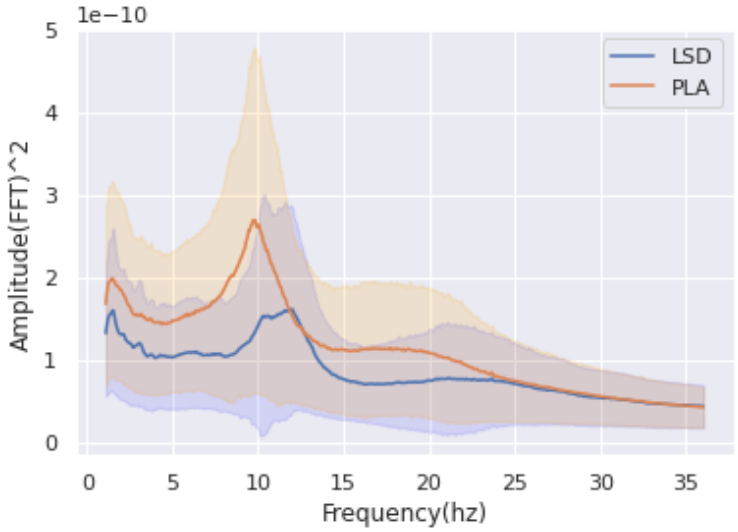

Fig. 3.1. Mean Power in LSD and Placebo

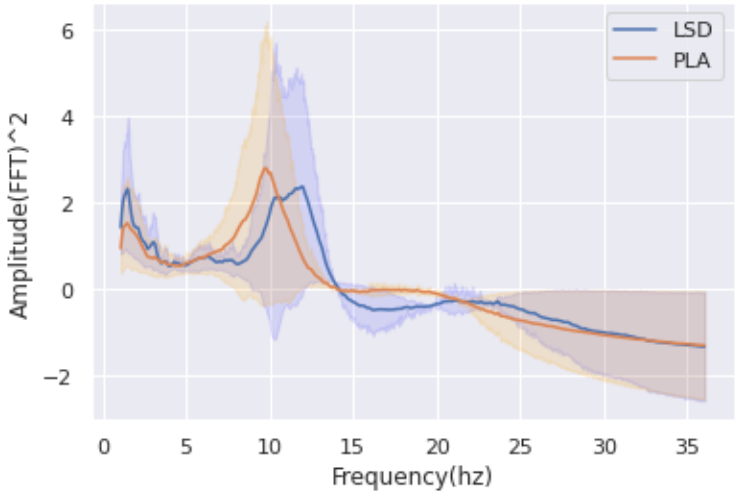

Fig. 3.2. Mean Power in LSD and Placebo Standardized

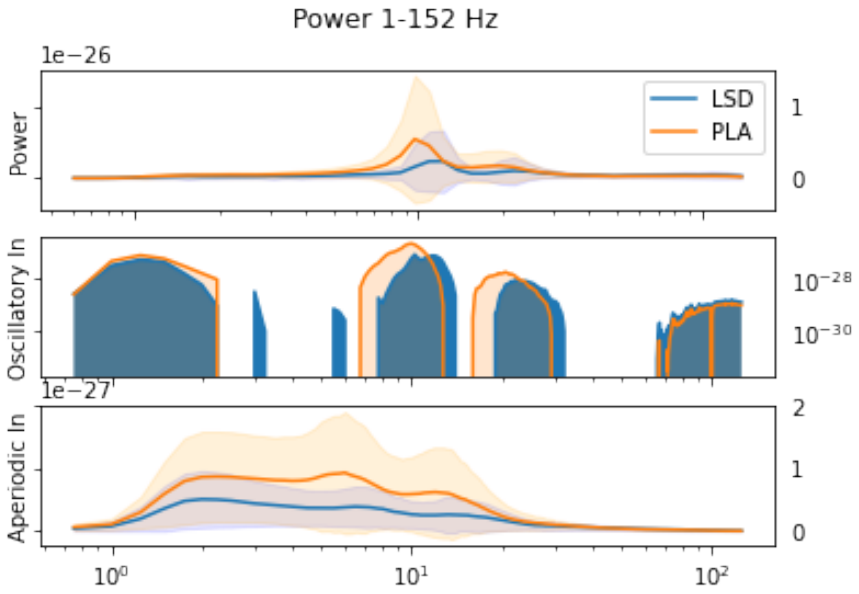

Fig. 3.3. Aperiodic and Oscillatory Power vs. Power

Contrary to previous findings, reported effects in sensor-level power (Muthukumaraswamy et al 2013; Carhart-Harris et al, 2016) were not consistent in direction. Nor were lower oscillatory decreases robust against multiple-comparisons. While uncorrected permutation statistics revealed consistent decreases in all lower frequencies, accompanied by increases in high gamma, multiple corrections revealed statistically robust increases in upper alpha , upper beta, gamma and high frequency oscillations, with decreases in theta/low-alpha, and low beta only. Among these, the only effects to endure when data were standardized to their respective conditions were increases in the upper frequencies of alpha and beta (both of whose frequency bins corresponded with peak increases under LSD)

	LSD	PLA
Alpha	11.2 ±1.4	10.1±1.3
Beta	23.2±4.2	19.1±3

Tableau 3.1. Average Peak Frequencies

Separate estimation of oscillatory and aperiodic power spectra revealed statistical significance across all frequencies in aperiodic spectrum, with increases in oscillatory gamma and decreases in all lower frequencies. This corresponds to a significant reduction in aperiodic slope under LSD as identified by FOOOF (see Fig. 3.7). Oscillatory effects were largely consistent with effects of baseline PSD (See Fig 3.3). Statistical comparison of peak alpha and beta identified a very robust peak shift in alpha and beta across all sensors (Significant with multiple comparisons p<=1e-10). This effect was robust in oscillatory, standardized

and non-standardized frequency spectra, and is quite pronounced in FOOOF-derived oscillations (see figure 3.5). Notably, oscillatory power derived by FOOOF was increased for beta and alpha oscillatory peaks. This finding completely contradicts previous findings with LSD electrophysiology, and attests to the overwhelming influence of cross-spectral changes in aperiodic slope.

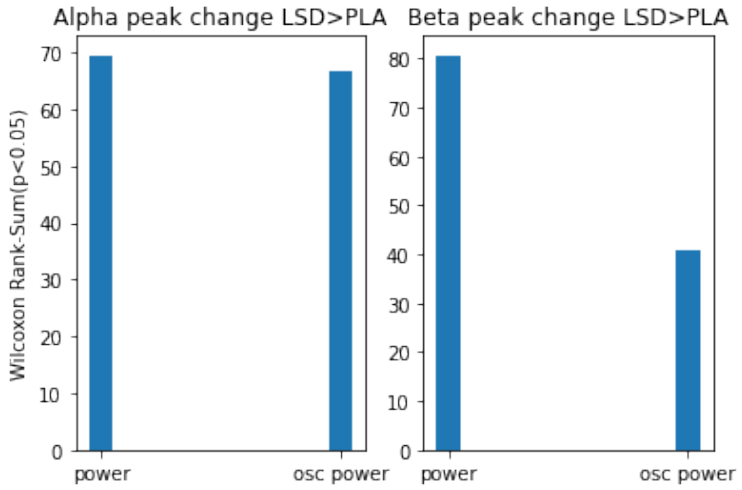

Fig. 3.4. Peak change statistics for Alpha and Beta

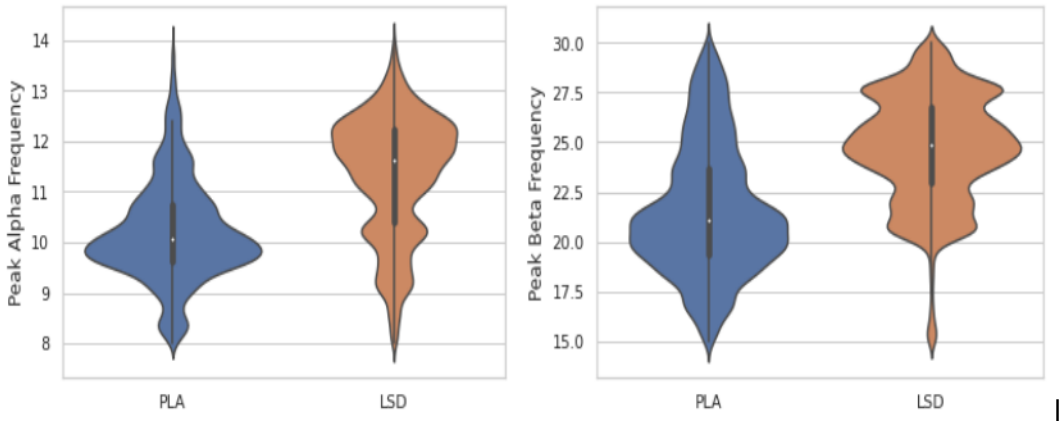

Fig. 3.5. Distribution of Alpha and Beta Peak Frequencies derived by FOOOF Algorithm

Source-level comparisons of non-standardized activity show alterations in peak frequency for alpha and beta were spatially consistent with many increases observed in power and connectivity. These effects were also consistent in extent when taking into account relative standard deviation in the frequency domain of the wavelet for "alpha" and "beta" frequencies respectively . In other words, degree of peak frequency increases were equivalent for alpha and beta given the intrinsic frequency resolution of the wavelet chosen.

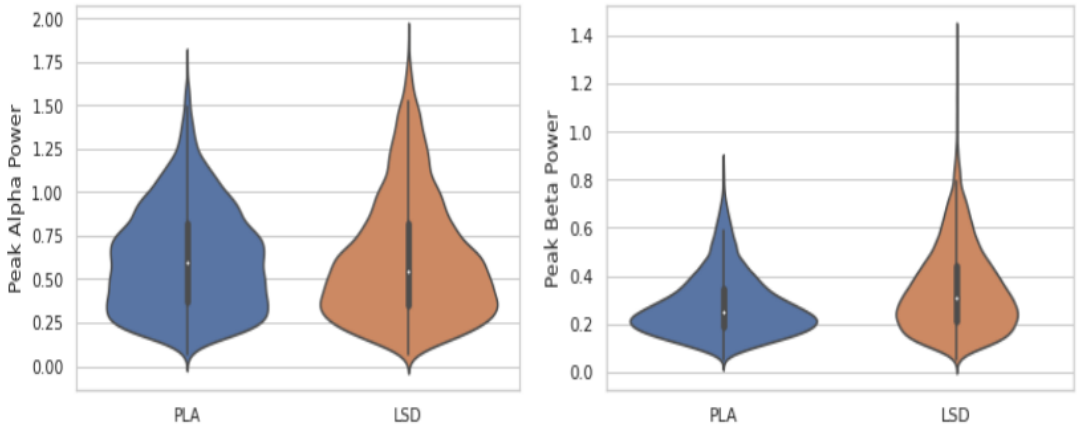

Fig. 3.6. Distribution of Alpha and Beta Peak Power derived by FOOOF Algorithm

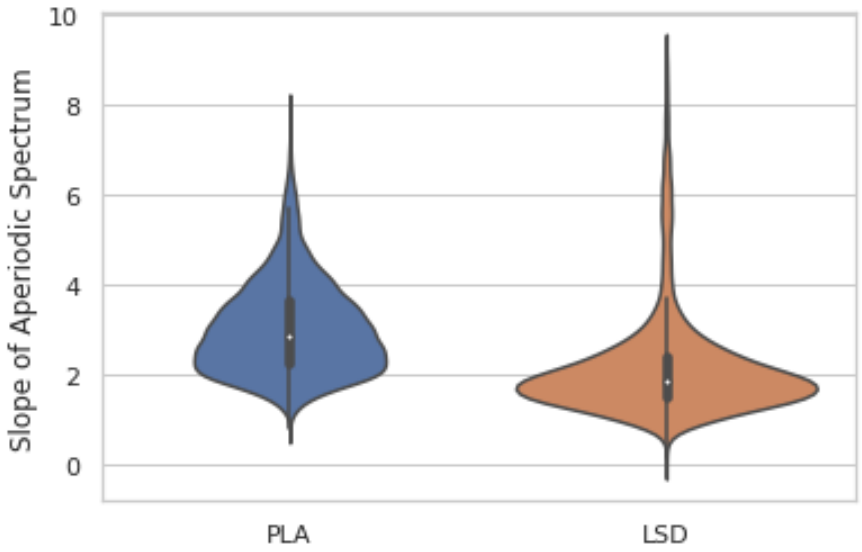

Fig. 3.7. Distribution of 1/f slope as derived by FOOOF Algorithm

3.2.2. Alterations in Connectivity under LSD

Initial identification of frequencies of interest controlled for multiple-comparisons revealed significant decreases in theta/low-alpha for both phase-based and amplitude-based coupling measures, decreases in low-beta for both phase and amplitude based coupling, and increases in high-alpha, high-beta and gamma. Unlike amplitude correlations, our phase based measure (PLI) revealed a significant increase in delta coupling. Notably only OAC identified a significant shift in peak alpha for mean connectivity over all sources, yet the increases in phase based coupling in high-alpha persist. Significance of effects by frequency are shown alongside mean connectivity by frequency for each condition in Figures 3.11 and 3.10

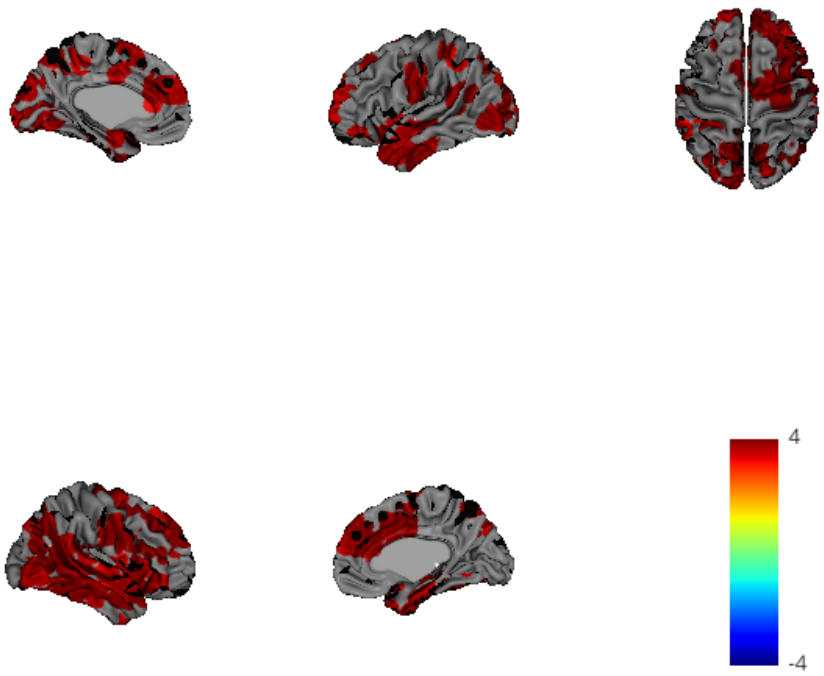

Fig. 3.8. Sources corresponding with alpha peak increases controlled for multiple comparisons

Alterations in Global Functional Connectivity (GFC, averaged connectivity) for brain-wide source within selected frequency ranges are shown in Appendix 1. Due to the convergence of frequencies identified by frequency selection procedure, and the frequency domain of peak increases–particularly alpha and beta–we also show statistical alterations taking only peak (high and low) frequencies into consideration for both alpha and beta.

3.2.3. Inter-regional Phase-Amplitude Coupling

Four clusters in paired phase-amplitude frequencies were identified using the same frequency identification procedure for interregional phase-amplitude coupling as outlined in the previous section. These frequencies were thresholded following a cluster permutation procedure outlined in the previous chapter which yielded clear bins.

Figure 3.14 shows commodulogram of significant increases connections each phase-amplitude bin for all inter-regional PAC connections. Figure 3.15 shows decreases. Clusters

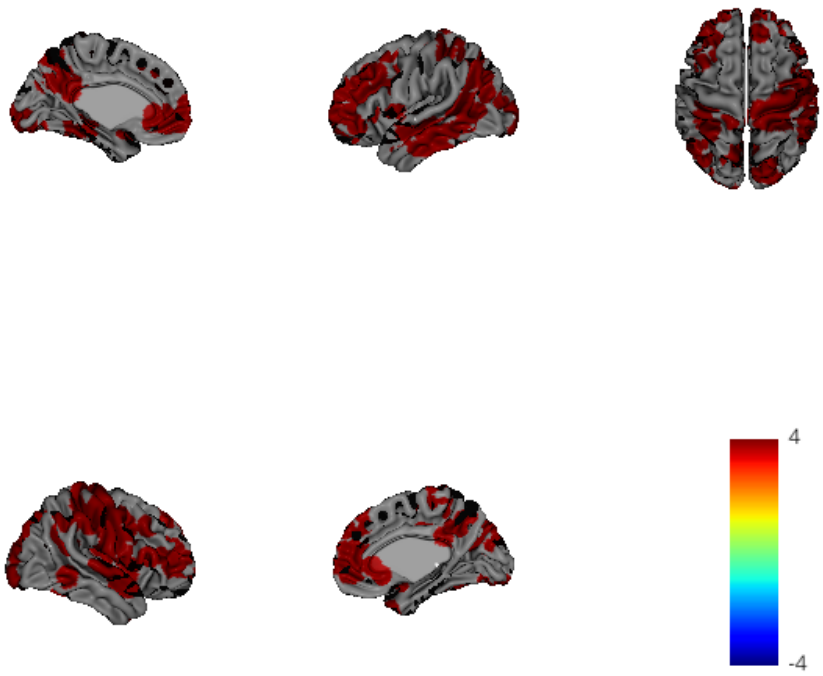

Fig. 3.9. Sources corresponding with beta peak increases controlled for multiple comparisons

of interest included a delta-alpha PAC cluster where coupling was seen to be increased under LSD (approx. 1 - 4 Hz phase with 9.75 hz amplitude center frequency), a delta-alpha cluster where PAC was shown to be decreased globally (approx. 1.5-6 hz phase paired with 12.5 hz amplitude center frequencies), a delta/theta-beta cluster increased under LSD (2-5hz phase and 17-22 hz amplitude), and a delta/theta-beta cluster decreasing under LSD (1-7 hz phase with 25-35hz amplitude). Figure 3.16 shows mean t-values of interregional pac. Both decreases and increases in delta-alpha coupling were most robust.

Source-wise global PAC values for phase and amplitude components of all significant connections in these identified clusters were derived. Source-wise effects in all significant clusters are included in Appendix 2

In order to better understand the relationship between these clusters. We compared locations where both increases and decreases were seen in corresponding clusters (suggesting a simple frequency shift of PAC effect), as well as regions where statistical matrices in the increase cluster bin corresponded to transposed version of matrices of statistical values in

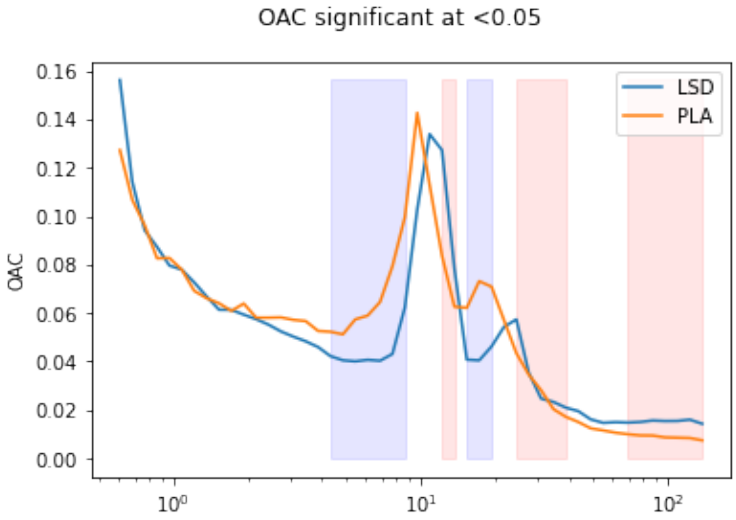

Fig. 3.10. Significant frequencies under multiple comparisons with mean values of LSD vs Placebo OAC

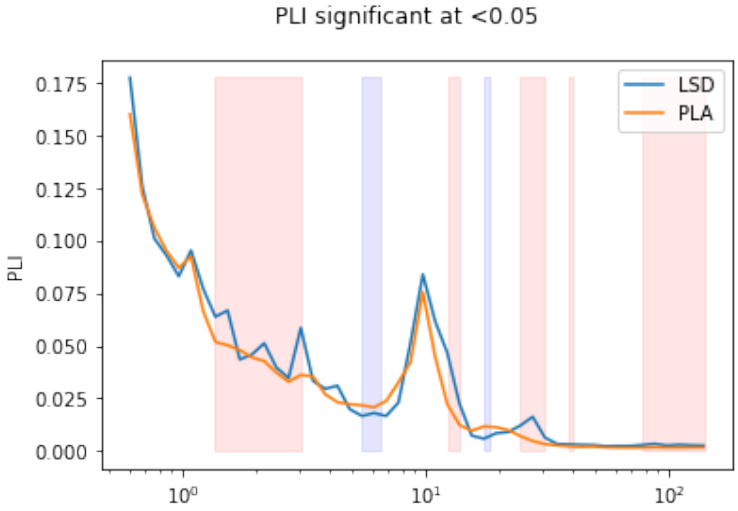

Fig. 3.11. Significant frequencies under multiple comparisons with mean values of LSD vs Placebo PLI

corresponding decrease bin (suggesting a reversal of phase-amplitude mediating effect in a given source).

We found that several of the regions identified as significant for both increased and decreased PAC under LSD were identical to regions previously identified as having a mediating role in LSD connectivity in fMRI (anterior cingulate, temporal lobe, auditory and visual cortices, sensorimotor network, medial, and inferior frontal cortices), suggesting a plausible shift in PAC frequency occurs in these areas.

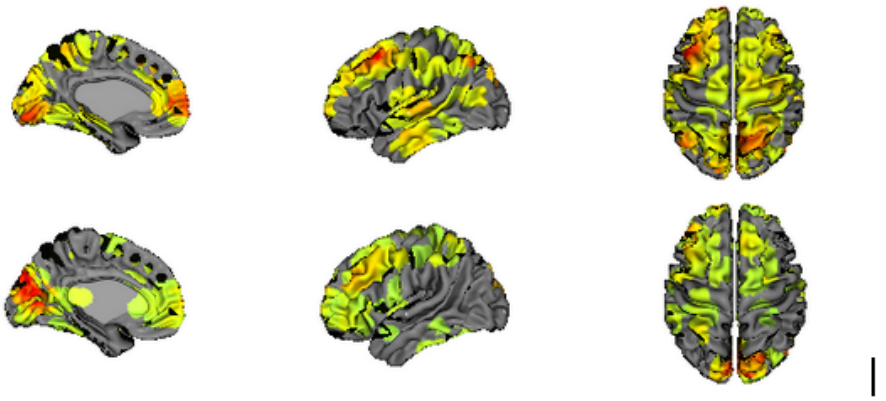

Fig. 3.12. Number of significant OAC connections per source (after MC) Top: Alpha; Bottom: Beta

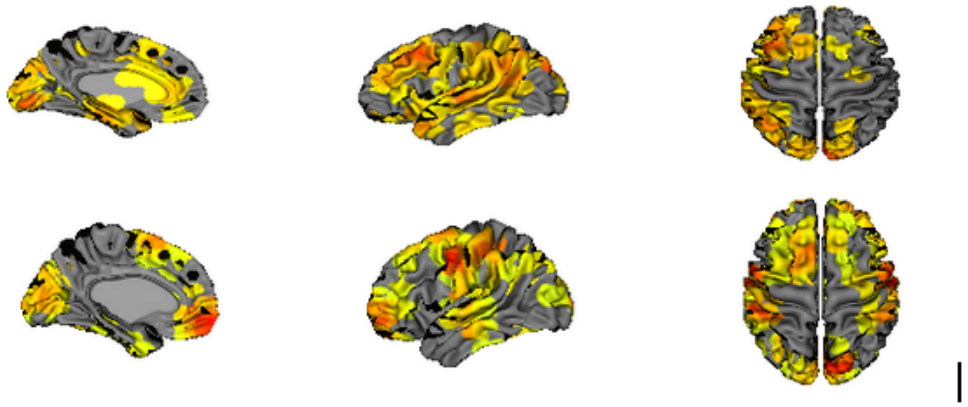

Fig. 3.13. Number of significant PLI connections per source (after MC) Top: Alpha; Bottom: Beta

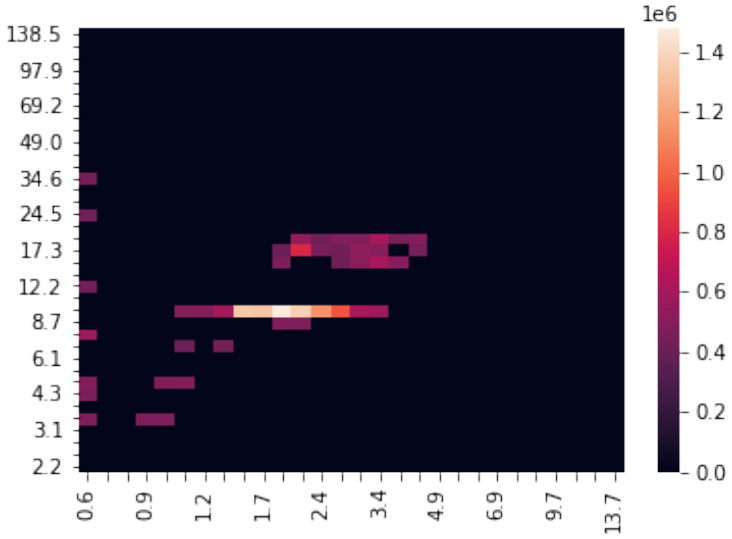

Fig. 3.14. Commodulogram showing phase-amplitude bins corresponding to significantly increased number of connections controlled for multiple comparisons

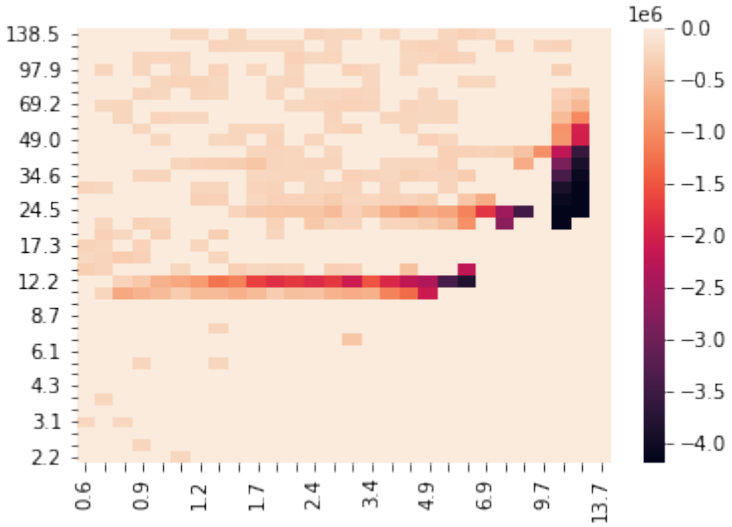

Fig. 3.15. Commodulogram showing phase-amplitude bins corresponding to significantly decreased number of connections controlled for multiple comparisons

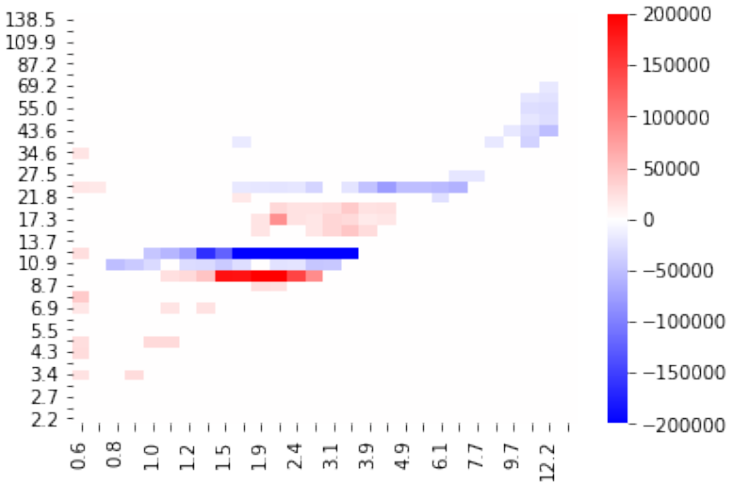

Fig. 3.16. Commodulogram showing phase-amplitude bins corresponding to mean (significant) t-values (Wilcoxon rank-sum) across decreased number of connections controlled for multiple comparisons

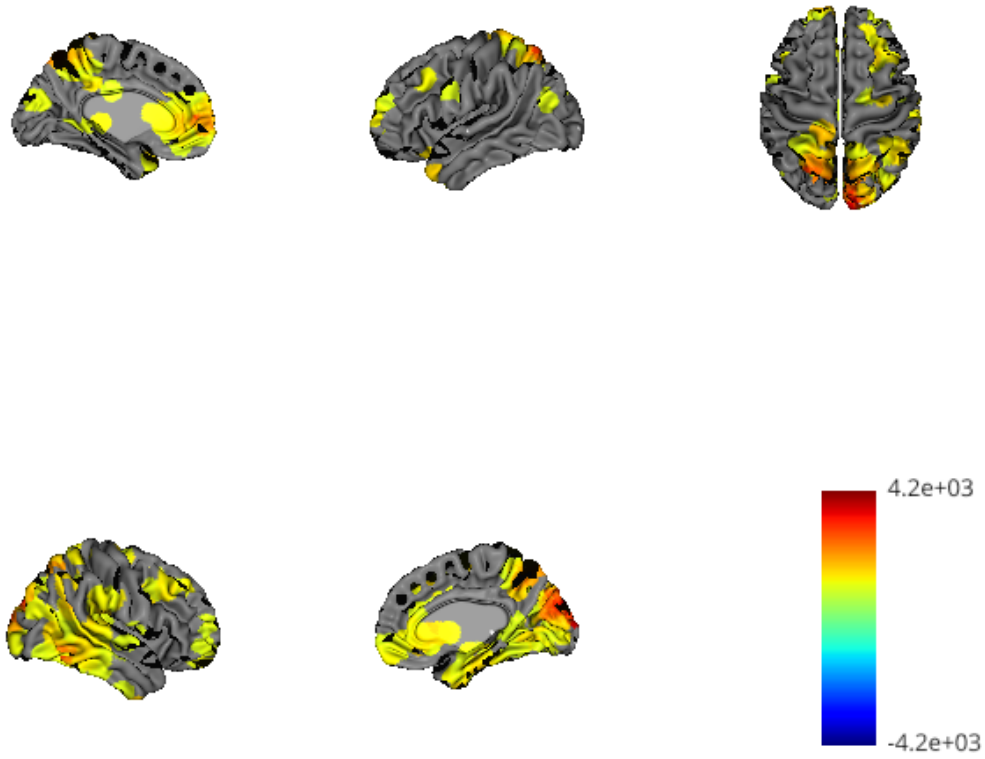

Fig. 3.17. Amplitude part of PAC shift in delta-alpha cluster under LSD

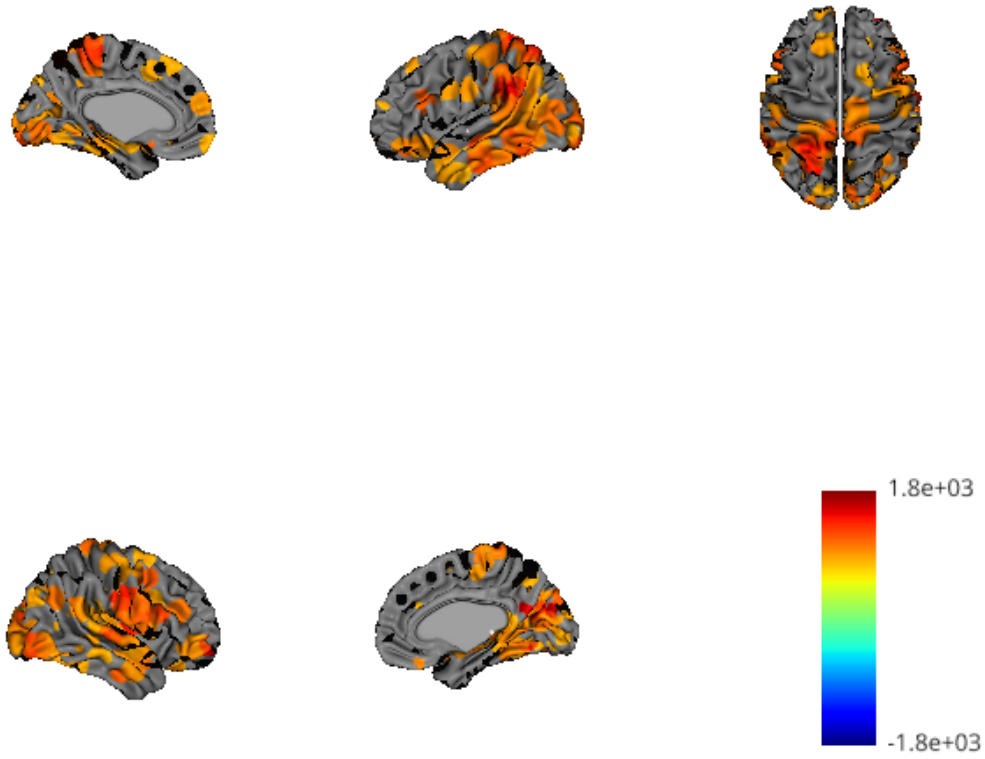

Fig. 3.18. Phase part of PAC frequency shift in delta-alpha cluster under LSD

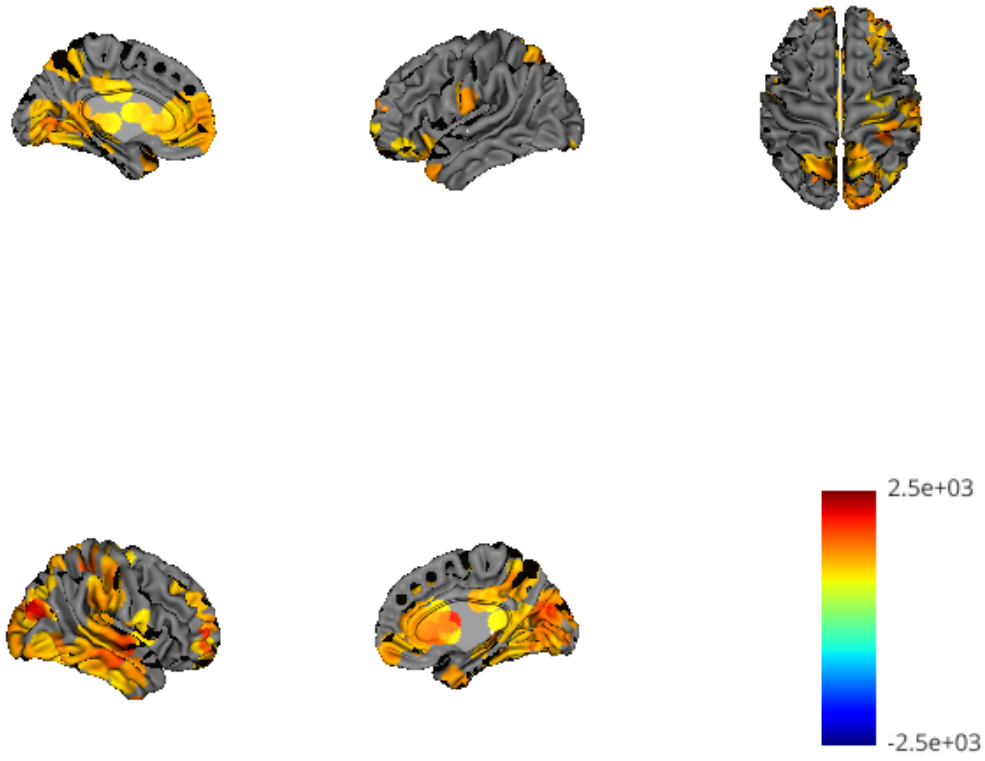

Fig. 3.19. Sources where phase sources were replaced by amplitude drivers under LSD in delta-alpha PAC

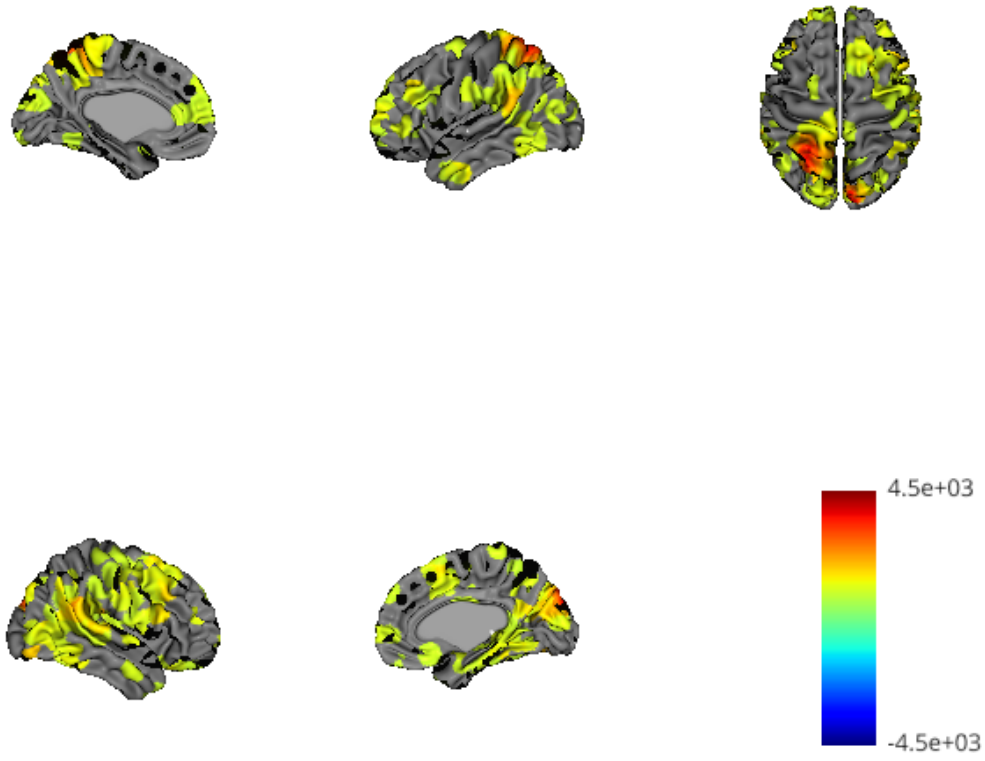

Fig. 3.20. Sources where amplitude drivers sources were replaced by phase sources under LSD in delta-alpha PAC

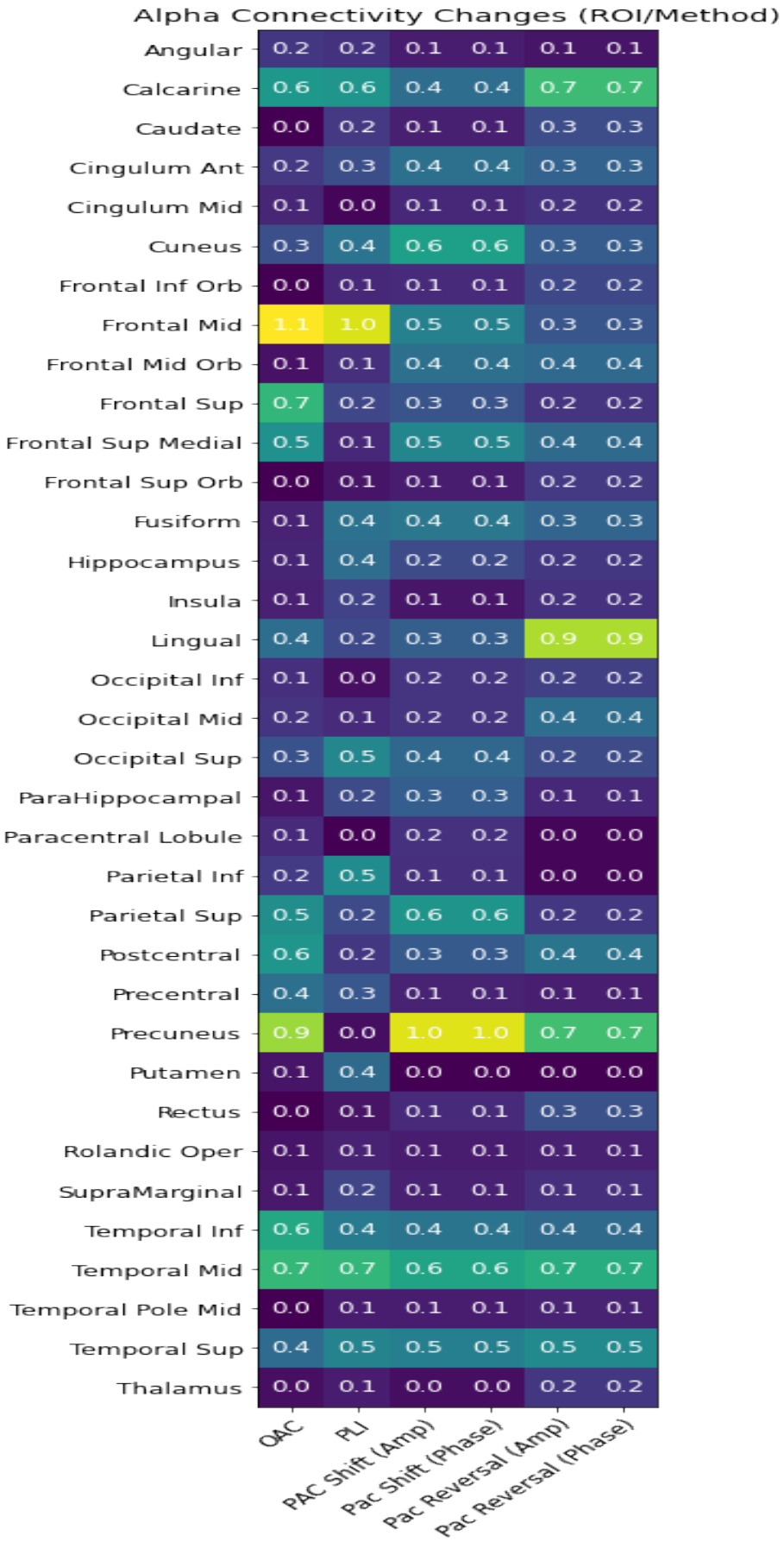

Fig. 3.21. Alpha Connectivity Results Across all Methods summarized using AAL ROIs

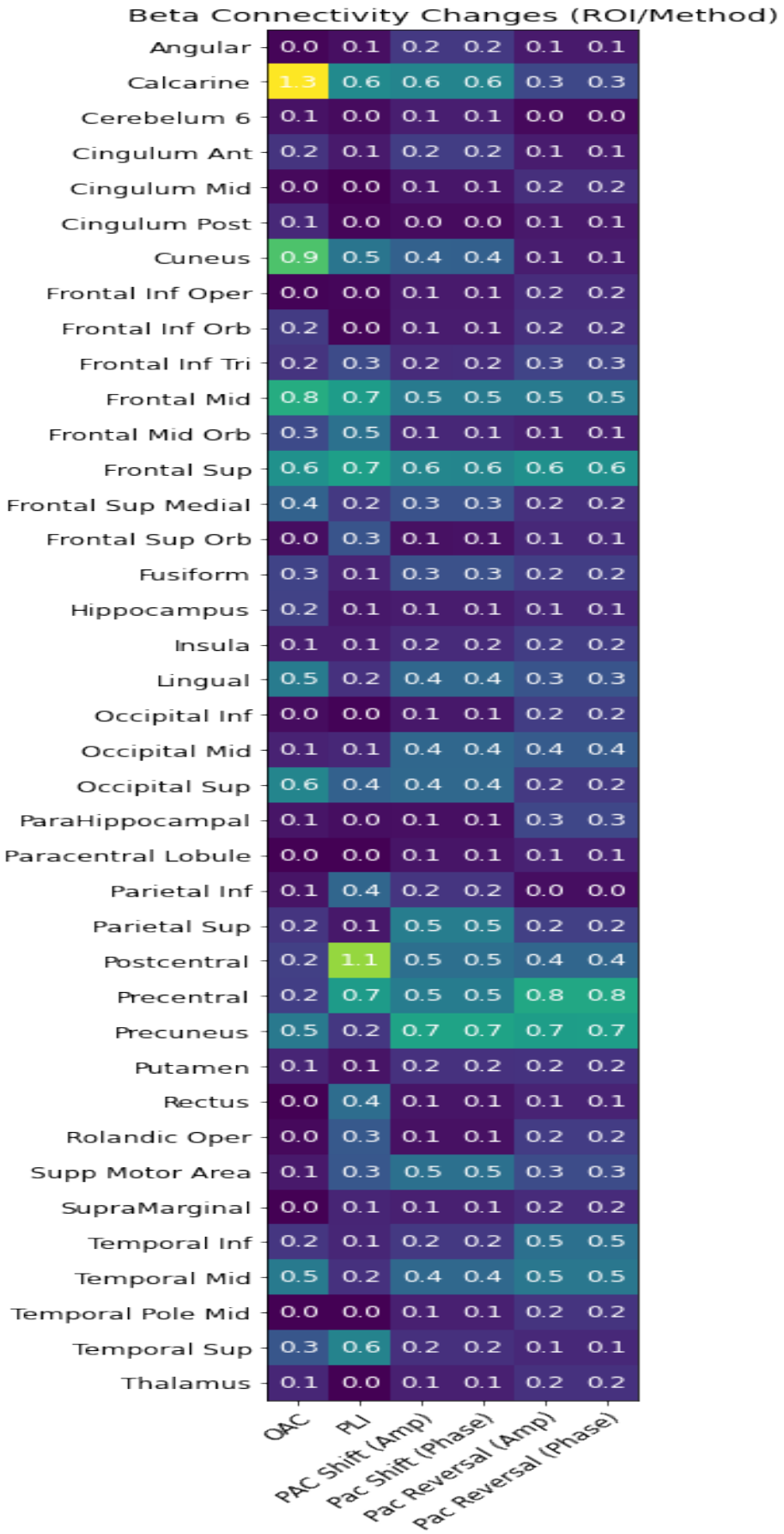

Fig. 3.22. Beta Connectivity Results Across all Methods summarized using AAL ROIs

Chapitre 4

Summary of Research and Conclusion

4.1. Discussion

The work presented here provides an intriguing albeit incomplete picture of the effects of LSD on whole-brain connectivity. From these results we can nevertheless draw several preliminary conclusions about the influence of LSD on electrophysiological coupling which might inform more mechanistically informed, and complete analyses of these effects in the future. The present chapter will proceed as follows. First we discuss spectral and connectivity results in light of existing literature on psychedelics in electrophysiological and BOLD-based studies of functional connectivity. We then discuss various aspects of the interregional PAC results, including the validity of our somewhat novel adaptive PAC method in light of observed results and extant literature. This is followed by a discussion of caveats and possible criticisms of our methodology, and a brief overview of promising future directions for this research.

From the spectral results outlined above, we can draw several important conclusions. First, shifts in peak frequency are robust, and impact not only alpha. Contrary to previously reported findings in electrophysiology, an upward shift in beta frequency was also observable in data. This effect was significant in resolved oscillatory, and standardized power spectra as well as simple power across sensors. From observed results it is also apparent that decreases in lower frequencies previously reported in electrophysiological literature on psychedelics (Muthukumaraswaky et al 2013; Carhart-Harris, et al 2016) can be largely accounted for by changes in baseline aperiodic power. They do not reflect relative alpha within a standardized frequency spectrum, nor an aperiodically regressed spectrum like FOOOF, but rather a displacement of the peak and trough of oscillatory alpha and beta. These displacements appear to influence coupling in power- as well as phase-based measures of synchronization, with reliable alterations in both phase and amplitude coupling corresponding to the peaks and troughs of oscillatory beta. Interestingly, oscillatory alpha does not exhibit increased, but decreased power in the upper alpha range where peak alpha increases are seen to be

largely expressed under LSD. Likewise oscillatory beta is seen to decrease in the upper beta region where peak is apparently displaced under LSD.

An interesting quality of PLI and OAC source level results is that they were largely non-overlapping in corresponding frequencies. However, increases in OAC for gamma, alpha and beta were partly spatially consistent, linking largely frontal, parietal and occipital cortices, as well as temporoparietal sources. Interestingly, this connectivity pattern was also partly observed in PLI's increases within the delta frequency bin. Any further consistency among PLI-based effects and OAC-based decreases across frequency would require additional analyses to elucidate. Importantly decreases and increases in corresponding oscillatory bands (e.g. beta decrease/increases) were not entirely overlapping, suggesting that the impact of LSD on coupling is not solely a reflection of observed displacement of oscillatory frequency.

The principal effect on PAC observed under LSD appears to reflect a downward shift in delta-alpha and delta-beta coupling in several regions highlighted as meaningful in previous literature (Tagliazucchi et al, 2016). This effect was also accompanied by an apparent switching of phase and amplitude in a number of regions. While both this ostensible shift and the possible reversal of phase-amplitude effects in some populations is intriguing, it would require further analyses to establish the statistical significance and possible functional meaning of this effect. Nandi et al. (2019) have provided strong evidence for the directed nature of interregional PAC, with (higher frequency) amplitude sources serving as a driver for slower-frequency instantaneous phase. In light of recent findings suggesting plausible alterations in the directionality of connectivity under psychedelics (Alamia et al, 2020; Barnett et al., 2020; Carhart-Harris & Friston, 2019; Preller et al., 2019), PAC based changes in directed CFC would make for an intriguing contribution to this mixed literature. However, any such interpretation of our data at this stage would be undoubtedly premature. Still, the application of some measure of directed coupling and/or Granger causality to sources identified at this preliminary stage (alongside more rigorous statistical testing) could help to elucidate the principal mechanisms at play. Another finding that warrants further investigation is the ostensibly inverse relationship between PAC frequency shifts and those identified in nearly all other modalities. Additional work must be done to elucidate the functional significance of this relationship.

4.1.1. Caveats

As stated previously, the results presented here are preliminary. Apart from this, several important points should be addressed. Firstly, given the criticisms of PAC, and the known presence of spurious PAC due to nonsinusoidal neural oscillations, is it possible that some or all of the observed CFC reported here could be epiphenomenal? We believe that the relatively low-frequency amplitudes corresponding to observed PAC changes suggest that these effects

are unlikely to be due to higher harmonics. Higher harmonics due to nonsinusoidal signal are generally assumed to be reflected in gamma and above, not in lower amplitude frequencies such as alpha and beta. Furthermore the correspondence of PAC increases to a frequency domain where power is decreased suggests that at the very least non-spurious PAC accounts for the changes seen under LSD (Jensen et al 2017). Because PAC is known to occur in distinct phase and amplitude populations, our interregional approach, combined with the application of SST, provides further evidence that PAC shift identified is likely non-spurious.

A second concern is the presence of significant changes in gamma power. While previous studies have identified legitimate changes in gamma accompanying psychedelics in intracranial EEG (Páleníček et al, 2013; Goda et al. 2013; Gonzalez et al 2020), results from scalp recordings of electrophysiological changes (Tofoli et al, 2016) have been readily dismissed on the basis that broadband gamma is known to overlap with the frequency spectrum of artifactual muscle activity (Muthukumaraswamy, 2013b; Muthukumaraswamy, 2013a; Carhart-Harris, 2016). Our study is much more concerned with increases observed in upper beta and alpha ranges, and did not observe PAC related increases in gamma. As such, we hesitate to draw definitive conclusions about the significance or validity of observed changes in gamma. Still the gamma increases observed in this study are a confound in light of previously reported changes in the power spectrum under psychedelics.

Finally, the usefulness and necessity of a wavelet-based IRASA implementation, and indeed the efficacy of IRASA itself relative to other proposed methods for separating 1/f and oscillatory frequency spectrum, such as FOOOF, should be addressed. We compared results from all three methods and found them to be largely consistent, with the caveat that a wavelet-based implementation requires significant tuning of time-frequency resolution, and ideally synchrosqueezing to achieve comparable resolution. This is largely due to the smearing of oscillatory peaks in frequency domain present in a time-frequency approach to spectral decomposition.

4.1.2. Future Directions

This work lends itself to a number of future directions, some of which have been discussed already. In addition to better statistical assessments of directedness of the PAC effect (via e.g. Granger causality), more detailed identification and seed-based connectivity analyses of regions of interest, and assessment of the relationship between displacement of the oscillatory spectrum and alterations in PAC frequencies, we propose extending the recently developed method of Alamia et al (2020) for detecting travelling alpha waves, to source-level regions of interest. In addition, dynamical connectivity is a matter of great interest. In addition to conventional measures of dynamic coupling, our proposed WIRASA method could be

applied to resolve amplitude-based connectivity in time for only rhythmic components of the frequency spectrum.

References

Abraham, H. D., & Duffy, F. H. (1996). Stable quantitative EEG difference in post-LSD visual disorder by split-half analysis: evidence for disinhibition. Psychiatry Research: Neuroimaging, 67(3), 173-187.

Adey, W. R., Bell, F. R., & Dennis, B. J. (1962). Effects of LSD-25, psilocybin and psilocin on temporal lobe EEG patterns & learned behavior in the cat. Neurology, 12(9), 591–602.

Alamia, A., & VanRullen, R. (2019). Alpha oscillations and traveling waves: Signatures of predictive coding?. PLoS Biology, 17(10), e3000487.

Alamia, A., Timmermann, C., Nutt, D. J., VanRullen, R., & Carhart-Harris, R. L. (2020). DMT alters cortical travelling waves. Elife, 9, e59784.

Anzolin, A., Presti, P., Van De Steen, F., Astolfi, L., Haufe, S., & Marinazzo, D. (2019). Quantifying the effect of demixing approaches on directed connectivity estimated between reconstructed EEG sources. Brain topography, 32(4), 655-674.

Attal, Y., & Schwartz, D. (2013). Assessment of subcortical source localization using deep brain activity imaging model with minimum norm operators: a MEG study. PLoS One, 8(3), e59856.

Auger, F., Flandrin, P., Lin, Y. T., McLaughlin, S., Meignen, S., Oberlin, T., & Wu, H. T. (2013). Time-frequency reassignment and synchrosqueezing: An overview. IEEE Signal Processing Magazine, 30(6), 32-41.

Bahramisharif, A., van Gerven, M. A., Aarnoutse, E. J., Mercier, M. R., Schwartz, T. H., Foxe, J. J., ... & Jensen, O. (2013). Propagating neocortical gamma bursts are coordinated by traveling alpha waves. Journal of Neuroscience, 33(48), 18849-18854.

Barnett, L., Muthukumaraswamy, S. D., Carhart-Harris, R. L., & Seth, A. K. (2020). Decreased directed functional connectivity in the psychedelic state. NeuroImage, 209, 116462.

Becker, D.I., Appel, J. B., Freedman, D.X.: Some effects of LSD on visual discrimination in pigeons. Psychopharmacologia (Berl.) 11, 354–364 (1967)

Bénar, C. G., Velmurugan, J., López-Madrona, V. J., Pizzo, F., & Badier, J. M. (2021). Detection and localization of deep sources in magnetoencephalography: a review. Current Opinion in Biomedical Engineering, 100285.

Berridge MJ, Prince WT. The nature of the binding between LSD and a 5-HT receptor: a possible explanation for hallucinogenic activity. Br J Pharmacol. 1974 Jun;51(2):269-78. doi: 10.1111/j.1476-5381.1974.tb09657.x. PMID: 4375525; PMCID: PMC1776744.

Berryman, R., Jarvik, M. E., Nevin, J. A.: Effects of pentobarbital, lysergie acid diethylamide and chlorpromazine on matching behavior in the pigeon. Psycho- pharmaeologia (Berl.) I , 60–65 (1962)

Blough, D. S. : Effect of lysergic acid diethylamide on absolute visual threshold of the pigeon. Science 126, 304–305 (1957a)

Blough, D. S. : Some effects of drugs on visual discrimination in the pigeon. Ann. N. Y. Acad. Sei. 66, 733–739 (1956)

Blough, D.S.: Effects of drugs on visually controlled behavior in pigeons. In: Psychotropie drugs. S. Garattini and V. Getti, Eds., pp. 110–118. Amserdam: Elsevier 1957b

Carhart-Harris, R. L., & Friston, K. J. (2019). REBUS and the anarchic brain: toward a unified model of the brain action of psychedelics. Pharmacological reviews, 71(3), 316-344.

Carhart-Harris, R. L., Muthukumaraswamy, S., Roseman, L., Kaelen, M., Droog, W., Murphy, K., ... & Nutt, D. J. (2016). Neural correlates of the LSD experience revealed by multimodal neuroimaging. Proceedings of the National Academy of Sciences, 113(17), 4853-4858.

Carhart-Harris, R. L., Erritzoe, D., Williams, T., Stone, J. M., Reed, L. J., Colasanti, A., ... & Nutt, D. J. (2012). Neural correlates of the psychedelic state as determined by fMRI studies with psilocybin

Carter, O. L., Hasler, F., Pettigrew, J. D., Wallis, G. M., Liu, G. B., & Vollenweider, F. X. (2007). Psilocybin links binocular rivalry switch rate to attention and subjective arousal levels in humans. Psychopharmacology, 195(3), 415-424.

Celada P,Puig MV, Díaz-Mataix L,Artigas F (2008) The hallucinogen DOI reduces low-frequency oscillations in rat prefrontal cortex: Reversal by antipsychotic drugs. Biol Psychiatry 64(5):392–400

Clark, C. R., Veltmeyer, M. D., Hamilton, R. J., Simms, E., Paul, R., Hermens, D., & Gordon, E. (2004). Spontaneous alpha peak frequency predicts working memory performance across the age span. International journal of psychophysiology, 53(1), 1-9.

Daubechies, I., Lu, J., & Wu, H. T. (2011). Synchrosqueezed wavelet transforms: An empirical mode decomposition-like tool. Applied and computational harmonic analysis, 30(2), 243-261.

Davis, M., & Sheard, M. H. (1975). Effects of lysergic acid diethylamide (LSD) on temporal recovery (pre-pulse inhibition) of the acoustic startle response in the rat. Pharmacology Biochemistry and Behavior, 3(5), 861-868.

Deco, G., Cruzat, J., Cabral, J., Knudsen, G. M., Carhart-Harris, R. L., Whybrow, P. C., ... & Kringelbach, M. L. (2018). Whole-brain multimodal neuroimaging model using serotonin receptor maps explains non-linear functional effects of LSD. Current biology, 28(19), 3065-3074.

Dellavale, D., Velarde, O. M., Mato, G., & Urdapilleta, E. (2020). Complex interplay between spectral harmonicity and different types of cross-frequency couplings in nonlinear oscillators and biologically plausible neural network models. Physical Review E, 102(6), 062401.

Donoghue T, Haller M, Peterson EJ, Varma P, Sebastian P, Gao R, Noto T, Lara AH, Wallis JD, Knight RT, Shestyuk A, & Voytek B (2020). Parameterizing neural power spectra into periodic and aperiodic components. Nature Neuroscience, 23, 1655-1665.

Dykstra, L.A., Appel, J.B. Effects of LSD on auditory perception: A signal detection analysis. Psychopharmacologia 34, 289–307 (1974). https://doi.org/10.1007/BF00422553

Fodor, Z., Marosi, C., Tombor, L., & Csukly, G. (2020). Salient distractors open the door of perception: alpha desynchronization marks sensory gating in a working memory task. Scientific reports, 10(1), 1-11.

Giehl, J., Noury, N., & Siegel, M. (2021). Dissociating harmonic and non-harmonic phase-amplitude coupling in the human brain. NeuroImage, 227, 117648.

Goda, S. A., Piasecka, J., Olszewski, M., Kasicki, S., & Hunt, M. J. (2013). Serotonergic hallucinogens differentially modify gamma and high frequency oscillations in the rat nucleus accumbens. Psychopharmacology, 228(2), 271-282.

Goda, S. A., Piasecka, J., Olszewski, M., Kasicki, S., & Hunt, M. J. (2013). Serotonergic hallucinogens differentially modify gamma and high frequency oscillations in the rat nucleus accumbens. Psychopharmacology, 228(2), 271-282.

Gonzalez, J., Cavelli, M., Castro-Zaballa, S., Mondino, A., Tort, A. B., Rubido, N., ... & Torterolo, P. (2020). Gamma band alterations and REM-like traits underpin the acute effect of the atypical psychedelic ibogaine. bioRxiv.

Haegens, S., Nácher, V., Luna, R., Romo, R., & Jensen, O. (2011). α-Oscillations in the monkey sensorimotor network influence discrimination performance by rhythmical inhibition of neuronal spiking. Proceedings of the National Academy of Sciences, 108(48), 19377-19382.

Halder, T., Talwar, S., Jaiswal, A. K., & Banerjee, A. (2019). Quantitative evaluation in estimating sources underlying brain oscillations using current source density methods and beamformer approaches. Eneuro, 6(4).

Hawellek, D. J., Schepers, I. M., Roeder, B., Engel, A. K., Siegel, M., & Hipp, J. F. (2013). Altered intrinsic neuronal interactions in the visual cortex of the blind. Journal of Neuroscience, 33(43), 17072-17080.

He, B. J., Zempel, J. M., Snyder, A. Z., & Raichle, M. E. (2010). The temporal structures and functional significance of scale-free brain activity. Neuron, 66(3), 353-369.

Hedrich, T., Pellegrino, G., Kobayashi, E., Lina, J. M., & Grova, C. (2017). Compar ison of the spatial resolution of source imaging techniques in high-density EEG and MEG. NeuroImage, 157, 531-544.

Herzog, R., Mediano, P. A., Rosas, F. E., Carhart-Harris, R., Perl, Y. S., Tagliazucchi, E., & Cofre, R. (2020). A mechanistic model of the neural entropy increase elicited by psychedelic drugs. Scientific reports, 10(1), 1-12.

Hipp, J. F., & Siegel, M. (2015). BOLD fMRI correlation reflects frequency-specific neuronal correlation. Current Biology, 25(10), 1368-1374.

Hipp, J. F., Hawellek, D. J., Corbetta, M., Siegel, M., & Engel, A. K. (2012). Large-scale cortical correlation structure of spontaneous oscillatory activity. Nature neuroscience, 15(6), 884-890.

Hoptman, M. J., Zuo, X. N., Butler, P. D., Javitt, D. C., D'Angelo, D., Mauro, C. J., & Milham, M. P. (2010). Amplitude of low-frequency oscillations in schizophrenia: a resting state fMRI study. Schizophrenia research, 117(1), 13-20.

Horovitz, Z. P., Mulroy, M. I., Waldron, T., & Leaf, R. (1965). Behavioral and electroencephalographic effects of LSD. Journal of pharmaceutical sciences, 54(1), 108-110.

Huang, N. E., & Wu, Z. (2008). A review on Hilbert-Huang transform: Method and its applications to geophysical studies. Reviews of geophysics, 46(2).

Jensen, O., Spaak, E., & Park, H. (2016). Discriminating valid from spurious indices of phase-amplitude coupling. Eneuro, 3(6).

Jiang, Q., & Suter, B. W. (2017). Instantaneous frequency estimation based on synchrosqueezing wavelet transform. Signal Processing, 138, 167-181.

Keil, J., Roa Romero, Y., Balz, J., Henjes, M., & Senkowski, D. (2016). Positive and negative symptoms in schizophrenia relate to distinct oscillatory signatures of sensory gating. Frontiers in human neuroscience, 10, 104.

Key, B. J.: The effect of drugs on discrimination and sensory generalization of auditory stimuli in cats. Psyehopharmacologia (Berl.) 2, 352–363 (1961)

Klimenko, S., Mitselmakher, G., & Sazonov, A. (2002). A cross-correlation technique in wavelet domain for detection of stochastic gravitational waves. arXiv preprint gr-qc/0208007.

Klimesch, W. (1997). EEG-alpha rhythms and memory processes. International Journal of psychophysiology, 26(1-3), 319-340.

Kovach, C. K., Oya, H., & Kawasaki, H. (2018). The bispectrum and its relationship to phase-amplitude coupling. Neuroimage, 173, 518-539.

Kraehenmann, R., Pokorny, D., Aicher, H., Preller, K. H., Pokorny, T., Bosch, O. G., ... & Vollenweider, F. X. (2017). LSD increases primary process thinking via serotonin 2A receptor activation. Frontiers in pharmacology, 8, 814.

Liley, D. T., & Muthukumaraswamy, S. D. (2020). Evidence that alpha blocking is due to increases in system-level oscillatory damping not neuronal population desynchronisation. NeuroImage, 208, 116408.

Lilly, J. M., & Olhede, S. C. (2012). Generalized Morse wavelets as a superfamily of analytic wavelets. IEEE Transactions on Signal Processing, 60(11), 6036-6041.

Liu, Y., San Liang, X., & Weisberg, R. H. (2007). Rectification of the bias in the wavelet power spectrum. Journal of Atmospheric and Oceanic Technology, 24(12), 2093-2102.

Lozano-Soldevilla, D. (2018). On the physiological modulation and potential mechanisms underlying par ieto-occipital alpha oscillations. Frontiers in computational neuroscience, 12, 23.

Mahjoory, K., Nikulin, V. V., Botrel, L., Linkenkaer-Hansen, K., Fato, M. M., & Haufe, S. (2017). Consistency of EEG source localization and connectivity estimates. Neuroimage, 152, 590-601.

Madsen, M. K., Fisher, P. M., Burmester, D., Dyssegaard, A., Stenbæk, D. S., Kristiansen, S., ... & Knudsen, G. M. (2019). Psychedelic effects of psilocybin correlate with serotonin 2A receptor occupancy and plasma psilocin levels. Neuropsychopharmacology, 44(7), 1328-1334.

McKenna, D. J., Nazarali, A. J., Hoffman, A. J., Nichols, D. E., Mathis, C. A., & Saavedra, J. M. (1989). Common receptors for hallucinogens in rat brain: a compar ative

autoradiographic study using [125I] LSD and [125I] DOI, a new psychotomimetic radioligand. Brain research, 476(1), 45-56.

Meignen, S., Oberlin, T., & McLaughlin, S. (2012). A new algorithm for multicomponent signals analysis based on synchrosqueezing: With an application to signal sampling and denoising. IEEE transactions on Signal Processing, 60(11), 5787-5798.

Mierau, A., Klimesch, W., & Lefebvre, J. (2017). State-dependent alpha peak frequency shifts: Experimental evidence, potential mechanisms and functional implications. Neuroscience, 360, 146-154.

Minuzzi, L., Nomikos, G. G., Wade, M. R., Jensen, S. B., Olsen, A. K., & Cumming, P. (2005). Interaction between LSD and dopamine D2/3 binding sites in pig brain. Synapse, 56(4), 198-204.

Müller, F., Dolder, P. C., Schmidt, A., Liechti, M. E., & Borgwardt, S. (2018). Altered network hub connectivity after acute LSD administration. NeuroImage: Clinical, 18, 694-701.

Munia, T. T., & Aviyente, S. (2019). Time-frequency based phase-amplitude coupling measure for neuronal oscillations. Scientific reports, 9(1), 1-15.

Murphy, K., & Fox, M. D. (2017). Towards a consensus regarding global signal regression for resting state functional connectivity MRI. Neuroimage, 154, 169-173.

Muthukumaraswamy, S. (2013). High-frequency brain activity and muscle artifacts in MEG/EEG: a review and recommendations. Frontiers in human neuroscience, 7, 138.

Muthukumaraswamy, S. D. (2014). The use of magnetoencephalography in the study of psychopharmacology (pharmaco-MEG). Journal of Psychopharmacology, 28(9), 815-829.

Nakada, M. T., Wieczorek, C. M., & Rainbow, T. C. (1984). Localization and characterization by quantitative autoradiography of [125I] LSD binding sites in rat brain. Neuroscience letters, 49(1-2), 13-18.

Nandi, B., Swiatek, P., Kocsis, B., & Ding, M. (2019). Inferring the direction of rhythmic neural transmission via inter-regional phase-amplitude coupling (ir-PAC). Scientific reports, 9(1), 1-13.

Nest, T. (2018). Coupling Mechanisms in LSD Electrophysiology. Oral Presentation at HBHL Research Meeting. McGill Montreal.

Nest, T., Deghan, A., Hipp, J., Muthukumaraswamy, S., Jerbi, K. (2019). Higher-Order Partial Least Squares Reveals Nuanced Changes in Pharmacological MEG. Poster Presentation at MAIN Conference. University of Montreal. Montreal

Nikulin, V. V., Jönsson, E. G., & Brismar, T. (2012). Attenuation of long-range temporal correlations in the amplitude dynamics of alpha and beta neuronal oscillations in patients with schizophrenia. Neuroimage, 61(1), 162-169.

Páleníček, T., Fujáková, M., Brunovský, M., Horáček, J., Gorman, I., Balíková, M., ... & Höschl, C. (2013). Behavioral, neurochemical and pharmaco-EEG profiles of the psychedelic drug 4-bromo-2, 5-dimethoxyphenethylamine (2C-B) in rats. Psychopharmacology, 225(1), 75-93.

Pallavicini, C., Vilas, M. G., Villarreal, M., Zamberlan, F., Muthukumaraswamy, S., Nutt, D., ... & Tagliazucchi, E. (2019). Spectral signatures of serotonergic psychedelics and glutamatergic dissociatives. NeuroImage, 200, 281-291.

Palva, S., & Palva, J. M. (2007). New vistas for α-frequency band oscillations. Trends in neurosciences, 30(4), 150-158.

Palva, J. M., Wang, S. H., Palva, S., Zhigalov, A., Monto, S., Brookes, M. J., ... & Jerbi, K. (2018). Ghost interactions in MEG/EEG source space: A note of caution on inter-areal coupling measures. Neuroimage, 173, 632-643.

Pang, J. C., & Robinson, P. A. (2018). Neural mechanisms of the EEG alpha-BOLD anticorrelation. Neuroimage, 181, 461-470.

Pang, Z., Alamia, A., & VanRullen, R. (2020). Turning the stimulus on and off dynamically changes the direction of alpha travelling waves. bioRxiv.

Pascual-Marqui, R. D. (2007). Discrete, 3D distributed, linear imaging methods of electric neuronal activity. Part 1: exact, zero error localization. arXiv preprint arXiv:0710.3341.

Petri G, et al. (2014) Homological scaffolds of brain functional networks.J R SocInterface11(101):20140873.19.

Piastra, M. C., Nüßing, A., Vorwerk, J., Clerc, M., Engwer, C., & Wolters, C. H. (2021). A comprehensive study on electroencephalography and magnetoencephalography sensitivity to cortical and subcortical sources. Human Brain Mapping, 42(4), 978-992.

Picco, P., Schiano, M. E., Incardone, S., Repetti, L., Demarte, M., Pensieri, S., & Bozzano, R. (2019). Detection and characterization of meteotsunamis in the Gulf of Genoa. Journal of Marine Science and Engineering, 7(8), 275.

Pittman-Polletta, B., Hsieh, W. H., Kaur, S., Lo, M. T., & Hu, K. (2014). Detecting phase-amplitude coupling with high frequency resolution using adaptive decompositions. Journal of neuroscience methods, 226, 15-32.

Posthuma, D., Neale, M. C., Boomsma, D. I., & De Geus, E. J. C. (2001). Are smarter brains running faster? Heritability of alpha peak frequency, IQ, and their interrelation. Behavior genetics, 31(6), 567-579.

Preller, K. H., Burt, J. B., Ji, J. L., Schleifer, C. H., Adkinson, B. D., Stämpfli, P., ... & Anticevic, A. (2018). Changes in global and thalamic brain connectivity in LSD-induced altered states of consciousness are attributable to the 5-HT2A receptor. Elife, 7, e35082.

Purpura, D. P. (1956). Electrophysiological analysis of psychotogenic drug action: I. Effect of LSD on specific afferent systems in the cat. AMA Archives of Neurology & Psychiatry, 75(2), 122-131.

Quednow, B. B., Kometer, M., Geyer, M. A., & Vollenweider, F. X. (2012). Psilocybin-induced deficits in automatic and controlled inhibition are attenuated by ketanserin in healthy human volunteers. Neuropsychopharmacology, 37(3), 630-640.

Recasens, M., Gross, J., & Uhlhaas, P. J. (2018). Low-frequency oscillatory correlates of auditory predictive processing in cortical-subcortical networks: a MEG-study. Scientific reports, 8(1), 1-12.

Ronconi, L., Busch, N. A., & Melcher, D. (2018). Alpha-band sensory entrainment alters the duration of temporal windows in visual perception. Scientific reports, 8(1), 1-10.

Sadaghiani, S., & Kleinschmidt, A. (2016). Brain networks and α-oscillations: structural and functional foundations of cognitive control. Trends in cognitive sciences, 20(11), 805-817.

Samaha, J., & Postle, B. R. (2015). The speed of alpha-band oscillations predicts the temporal resolution of visual perception. Current Biology, 25(22), 2985-2990.

Schartner, M. M., Carhart-Harris, R. L., Barrett, A. B., Seth, A. K., & Muthukumaraswamy, S. D. (2017). Increased spontaneous MEG signal diversity for psychoactive doses of ketamine, LSD and psilocybin. Scientific reports, 7(1), 1-12.

Schmidt, A., Müller, F., Lenz, C., Dolder, P. C., Schmid, Y., Zanchi, D., ... & Borgwardt, S. (2018). Acute LSD effects on response inhibition neural networks. Psychol Med, 48(9), 1464-73.

Schwartz, A. S., & Cheney, C. (1965). Effect of LSD on the tonic activity of the visual pathways of the cat. Life Sciences, 4(7), 771–778.

Seeman, P., Ko, F., & Tallerico, T. (2005). Dopamine receptor contribution to the action of PCP, LSD and ketamine psychotomimetics. Molecular psychiatry, 10(9), 877-883.

Sekihara, K., Sahani, M., & Nagarajan, S. S. (2005). Localization bias and spatial resolution of adaptive and non-adaptive spatial filters for MEG source reconstruction. Neuroimage, 25(4), 1056-1067.

Shagass, C. (1967). Effects of LSD on somatosensory and visual evoked responses and on the EEG in man. Recent advances in biological psychiatry, 209-227.

Sharpe, L. B., Otis, L. S., Schnsterman, R. S. : Disruption of size discrimination in squirrel monkeys by LSD-25. Psyehon. Sei. 7, 103–104 (1967)

Siddik, Z. H., Barnes, R. D., Dring, L. G., Smith, R. L., & Williams, R. T. (1979). The fate of lysergic acid DI [14C] ethylamide ([14C] LSD) in the rat, guinea pig and rhesus monkey and of [14C] iso-LSD in rat. Biochemical pharmacology, 28(20), 3093-3101.

Siegel, R. K. : Effects of cannabis sativa and lysergie acid diethylamide on a visual discrimination task in pigeons. Psychopharmacologia (Berl.) 15, 1–8 (1969)

Sotero, R. C. (2015b). Modeling the generation of phase-amplitude coupling in cortical circuits: From detailed networks to neural mass models. BioMed research international, 2015.

Sotero, R. C., Bortel, A., Naaman, S., Mocanu, V. M., Kropf, P., Villeneuve, M. Y., & Shmuel, A. (2015a). Laminar distribution of phase-amplitude coupling of spontaneous current sources and sinks. Frontiers in neuroscience, 9, 454.

Spaak, E., de Lange, F. P., & Jensen, O. (2014). Local entrainment of alpha oscillations by visual stimuli causes cyclic modulation of perception. Journal of Neuroscience, 34(10), 3536-3544.

Strogatz S.H. (1994) Norbert Wiener's Brain Waves. In: Levin S.A. (eds) Frontiers in Mathematical Biology. Lecture Notes in Biomathematics, vol 100. Springer, Berlin, Heidelberg.

Stuckey, D. E., Lawson, R., & Luna, L. E. (2005). EEG gamma coherence and other correlates of subjective reports during ayahuasca experiences. Journal of psychoactive drugs, 37(2), 163-178.

Tagliazucchi E, Carhart-Harris R, Leech R, Nutt D, Chialvo DR (2014) Enhanced rep-ertoire of brain dynamical states during the psychedelic experience.Hum Brain Mapp35:5442–5456

Tagliazucchi, E., Roseman, L., Kaelen, M., Orban, C., Muthukumaraswamy, S. D., Murphy, K., & Carhart-Harris, R. (2016). Increased global functional connectivity correlates with LSD-induced ego dissolution. Current Biology, 26(8), 1043-1050.

Thoma, R. J., Hanlon, F. M., Moses, S. N., Ricker, D., Huang, M., Edgar, C., ... & Canive, J. M. (2005). M50 sensory gating predicts negative symptoms in schizophrenia. Schizophrenia research, 73(2-3), 311-318.

Timmermann, C., Roseman, L., Schartner, M., Milliere, R., Williams, L. T., Erritzoe, D., ... & Carhart-Harris, R. L. (2019). Neural correlates of the DMT experience assessed with multivariate EEG. Scientific reports, 9(1), 1-13.

Tófoli, L. F., & de Araujo, D. B. (2016). Treating addiction: Perspectives from EEG and imaging studies on psychedelics. International review of neurobiology, 129, 157-185.

Tsai, F. F., Fan, S. Z., Cheng, H. L., & Yeh, J. R. (2019). Multi-timescale phase-amplitude couplings in transitions of anesthetic-induced unconsciousness. Scientific reports, 9(1), 1-11.

Tsang, K. W., Ghosh, A., Samajdar, A., Chatziioannou, K., Mastrogiovanni, S., Agathos, M., & Van Den Broeck, C. (2020). A morphology-independent search for gravitational wave echoes in data from the first and second observing runs of Advanced LIGO and Advanced Virgo. Physical Review D, 101(6), 064012.

Uhlhaas, P. J., & Singer, W. (2010). Abnormal neural oscillations and synchrony in schizophrenia. Nature reviews neuroscience, 11(2), 100-113.

van der Meer, J., & Breakspear, M. (2018). Neuroscience: Modeling the Brain on Acid. Current Biology, 28(19), R1157-R1160.

VanRullen, R., & Koch, C. (2003). Is perception discrete or continuous?. Trends in cognitive sciences, 7(5), 207-213.

Varley, T. F., Carhart-Harris, R., Roseman, L., Menon, D. K., & Stamatakis, E. A. (2020). Serotonergic psychedelics LSD & psilocybin increase the fractal dimension of cortical brain activity in spatial and temporal domains. NeuroImage, 220, 117049.

Vinck, M., Oostenveld, R., Van Wingerden, M., Battaglia, F., & Pennartz, C. M. (2011). An improved index of phase-synchronization for electrophysiological data in the presence of volume-conduction, noise and sample-size bias. Neuroimage, 55(4), 1548-1565.

Vollenweider FX, et al. (1997) Positron emission tomography and fluorodeoxyglucose-studies of metabolic hyperfrontality and psychopathology in the psilocybin model ofpsychosis.Neuropsychopharmacology16(5):357–372.

Vollenweider FX, Vollenweider-Scherpenhuyzen MFI, Bäbler A, Vogel H, Hell D . (1998): Psilocybin induces schizophrenia-like psychosis in humans via a serotonin-2 agonist action. NeuroReport 9: 3897–3902

Vollenweider, F. X., Vontobel, P., Hell, D., & Leenders, K. L. (1999). 5-HT modulation of dopamine release in basal ganglia in psilocybin-induced psychosis in man—a PET study with [11 C] raclopride. Neuropsychopharmacology, 20(5), 424-433.

Wen, H., & Liu, Z. (2016). Separ ating fractal and oscillatory components in the power

spectrum of neurophysiological signal. Brain topography, 29(1), 13-26.

Wens, V., Marty, B., Mary, A., Bourguignon, M., Op de Beeck, M., Goldman, S., ... & De Tiège, X. (2015). A geometric correction scheme for spatial leakage effects in MEG/EEG seed-based functional connectivity mapping. Human brain mapping, 36(11), 4604-4621.

Wipf, D. P., Owen, J. P., Attias, H. T., Sekihara, K., & Nagarajan, S. S. (2010). Robust Bayesian estimation of the location, orientation, and time course of multiple correlated neural sources using MEG. NeuroImage, 49(1), 641-655.

Wong, D. F., Lever, J. R., Hartig, P. R., Dannals, R. F., Villemagne, V., Hoffman, B. J., ... & Wagner Jr, H. N. (1987). Localization of serotonin 5-HT2 receptors in living human brain by positron emission tomography using N1-([11C]-methyl)-2-BR-LSD. Synapse, 1(5), 393-398.

Wood J,Kim Y,Moghaddam B (2012) Disruption of prefrontal cortex large scale neuronal activity by different classes of psychotomimetic drugs. J Neurosci 32(9):3022–3031

Wu, H. T., Flandrin, P., & Daubechies, I. (2011). One or two frequencies? The synchrosqueezing answers. Advances in Adaptive Data Analysis, 3(01n02), 29-39.

Yeh, C. H., & Shi, W. (2018). Identifying phase-amplitude coupling in cyclic alternating pattern using masking signals. Scientific reports, 8(1), 1-9.

Yeh, C. H., Lo, M. T., & Hu, K. (2016). Spurious cross-frequency amplitude–amplitude coupling in nonstationary, nonlinear signals. Physica A: Statistical Mechanics and its Applications, 454, 143-150.

Zhang, H., Watrous, A. J., Patel, A., & Jacobs, J. (2018). Theta and alpha oscillations are traveling waves in the human neocortex. Neuron, 98(6), 1269-1281.

Zhao, Q., Caiafa, C. F., Mandic, D. P., Chao, Z. C., Nagasaka, Y., Fujii, N., ... & Cichocki, A. (2012). Higher order par tial least squares (HOPLS): a generalized multilinear regression method. IEEE transactions on pattern analysis and machine intelligence, 35(7), 1660-1673.

Annexe A

Sensor Level FOOOF Results

A.1. Aggregate Results for Sensor-Level PSDs

A.2. FOOOF Group Results for Sensor-Level PSDs

```
==============================================================================================

                                FOOOF - POWER SPECTRUM MODEL

                The model was run on the frequency range 0 - 49 Hz
                        Frequency Resolution is 0.17 Hz

                 Aperiodic Parameters (offset, knee, exponent):
                           -24.8769, 411.8804, 2.1129

                                  5 peaks were found:
                        CF:   1.74, PW:  0.263, BW:  1.00
                        CF:   3.02, PW:  0.083, BW:  1.00
                        CF:  10.72, PW:  0.463, BW:  2.27
                        CF:  12.46, PW:  0.396, BW:  1.44
                        CF:  23.32, PW:  0.201, BW:  5.33

                                Goodness of fit metrics:
                               R^2 of model fit is 0.9839
                               Error of the fit is 0.0268

==============================================================================================
```

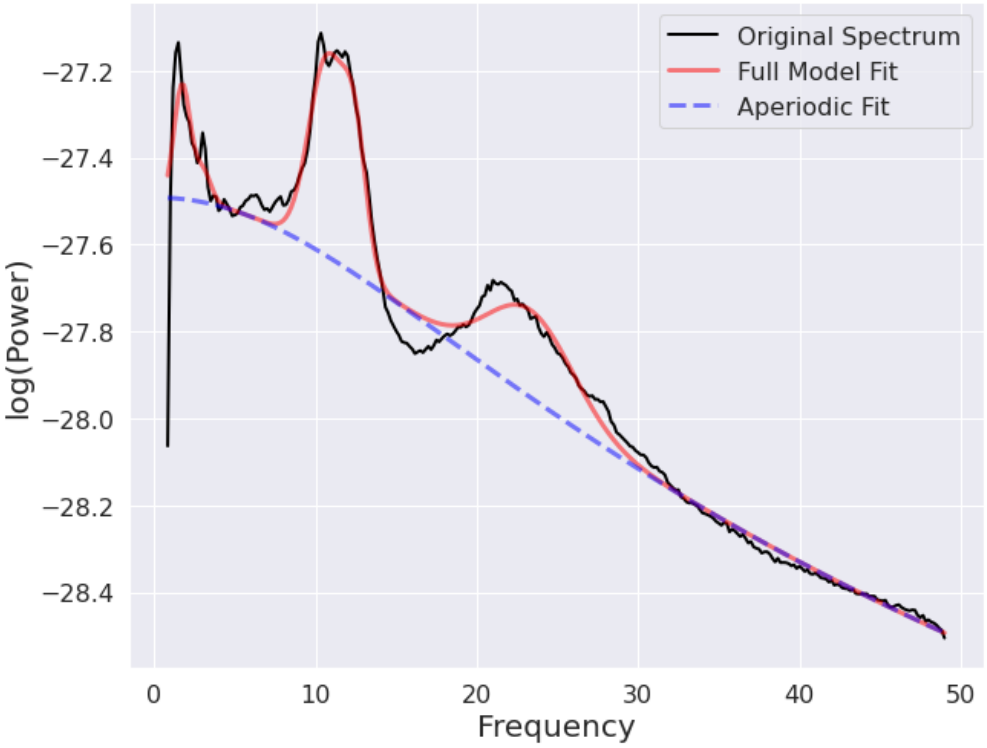

Fig. A.1. FOOOF fit for mean LSD spectrum

```
================================================================================================

                                FOOOF - POWER SPECTRUM MODEL

                The model was run on the frequency range 0 - 49 Hz
                        Frequency Resolution is 0.17 Hz

                 Aperiodic Parameters (offset, knee, exponent):
                           -23.4787, 5309.7432, 3.0322

                                  3 peaks were found:
                        CF:   1.88, PW:  0.205, BW:  1.00
                        CF:   9.84, PW:  0.517, BW:  2.65
                        CF:  20.64, PW:  0.144, BW:  4.34

                                Goodness of fit metrics:
                               R^2 of model fit is 0.9886
                               Error of the fit is 0.0350

================================================================================================
```

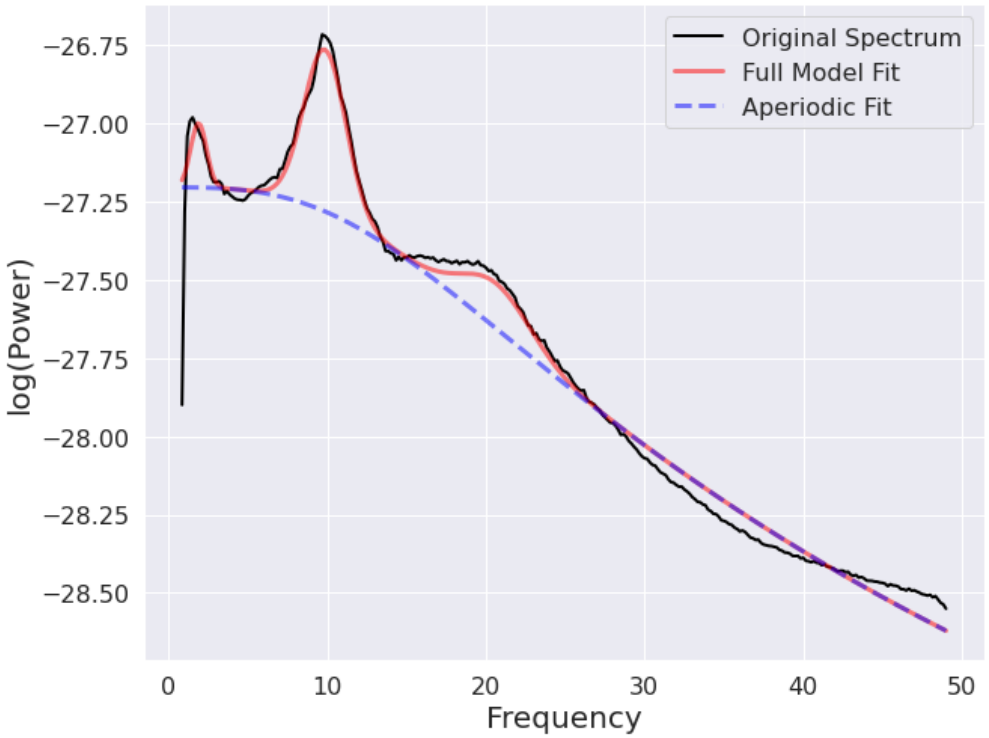

Fig. A.2. FOOOF output for mean PLA spectrum

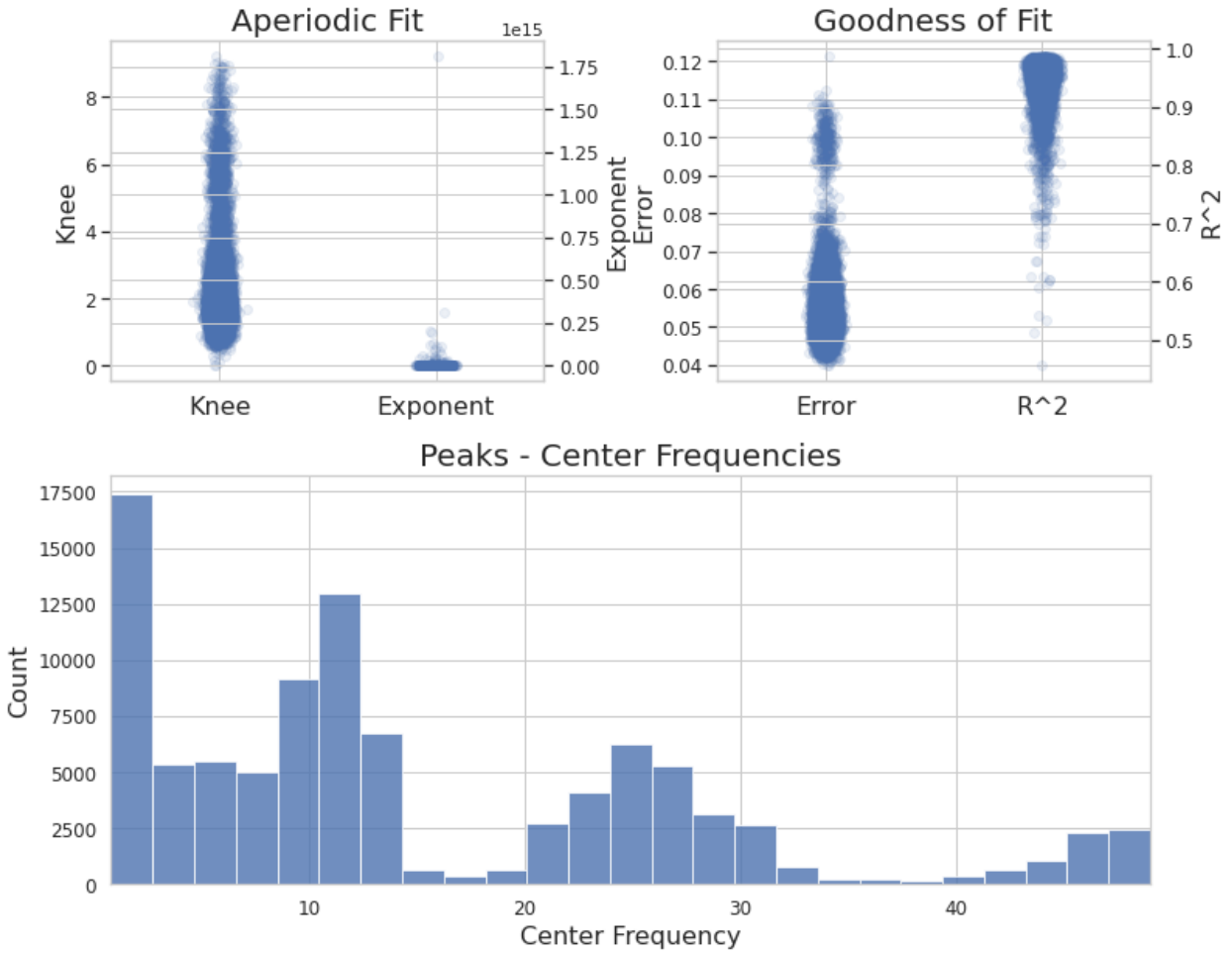

Fig. A.3. FOOOF Group output for ALL LSD Sensors

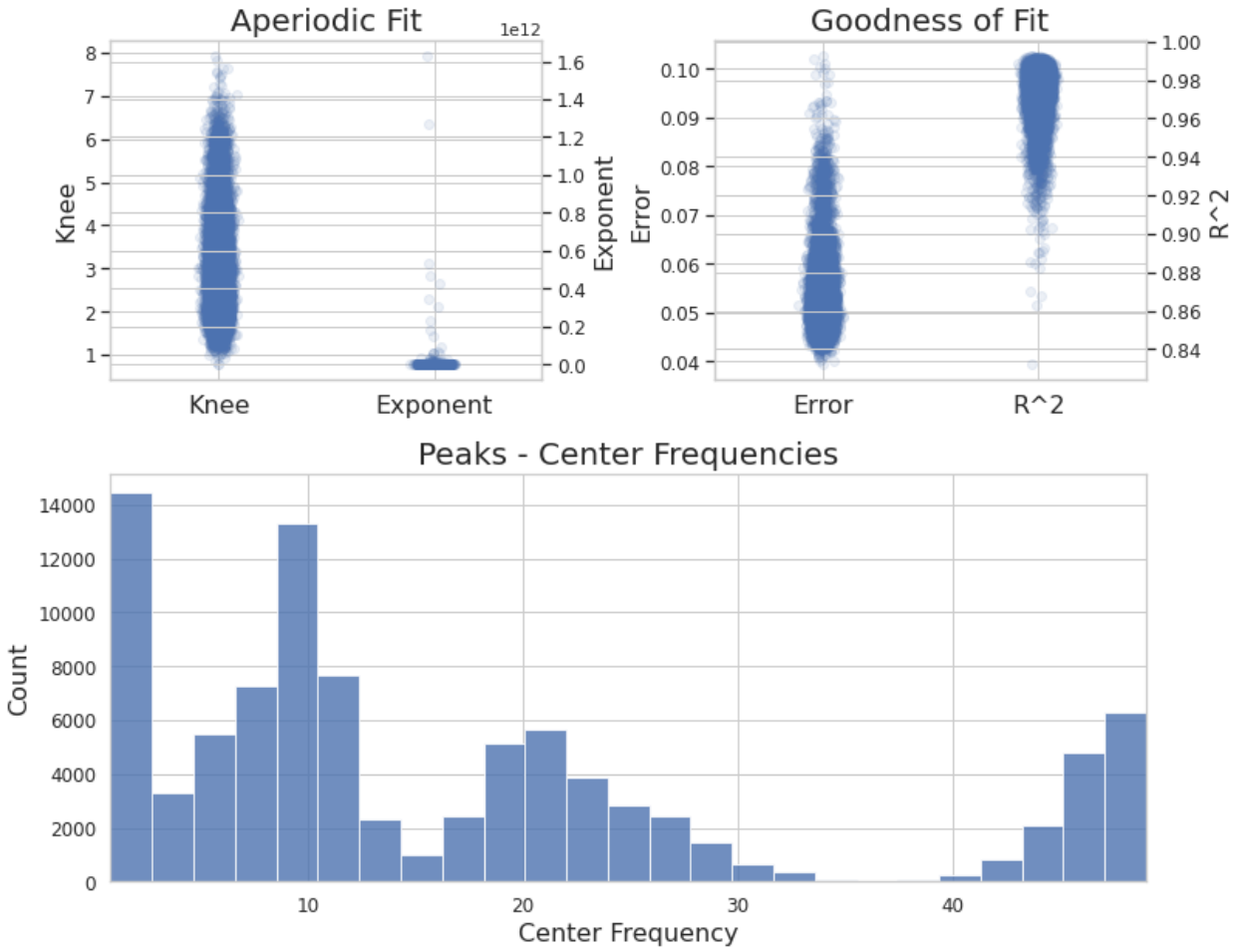

Fig. A.4. FOOOF Group output for ALL PLA Sensors

Annexe B

Source Level Connectivity of PLI and OAC

B.1. Connectivity changes as measured by PLI

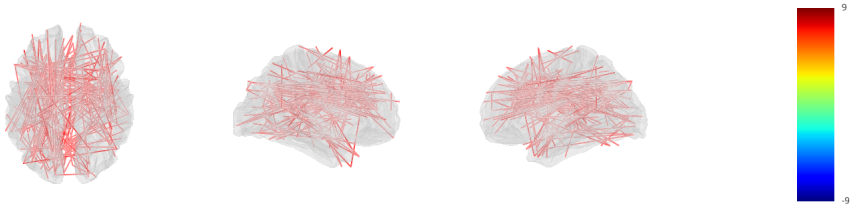

Fig. B.1. Changes in PLI in significant delta bin (Wilcoxon rank-sum, p<=1e-10)

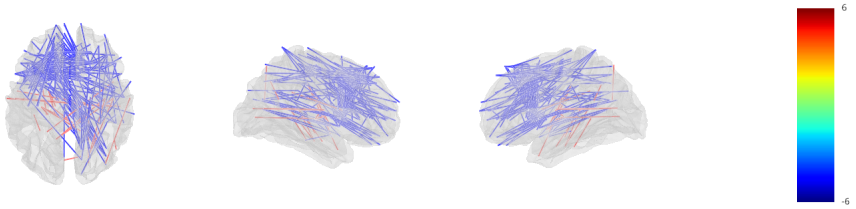

Fig. B.2. Changes in PLI in significant theta bin (Wilcoxon rank-sum, p<=1e-10)

B.2. Connectivity changes as measured by OAC

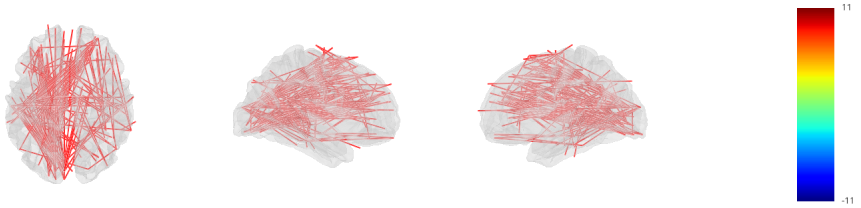

Fig. B.3. Changes in PLI in significant alpha bin (Wilcoxon rank-sum, p<=1e-10)

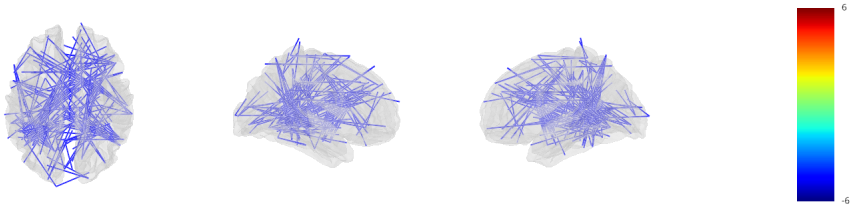

Fig. B.4. Changes in PLI in significant lower beta bin (Wilcoxon rank-sum, p<=1e-10)

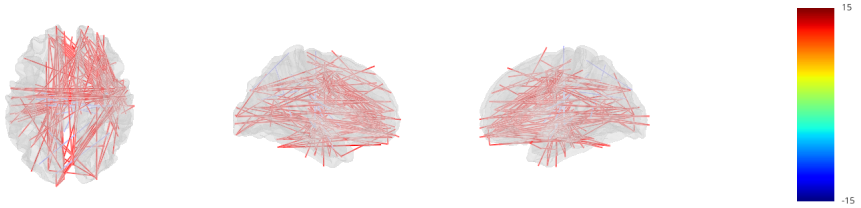

Fig. B.5. Changes in PLI in significant upper beta bin (Wilcoxon rank-sum, p<=1e-10)

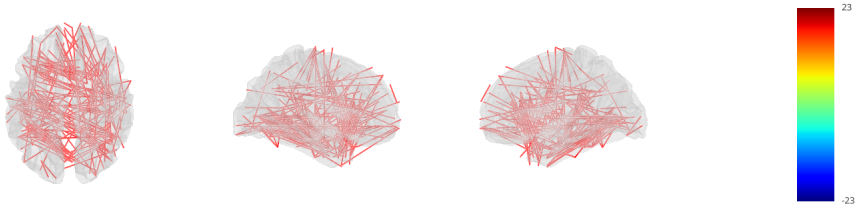

Fig. B.6. Changes in PLI in significant gamma bin (Wilcoxon rank-sum, p<=1e-10)

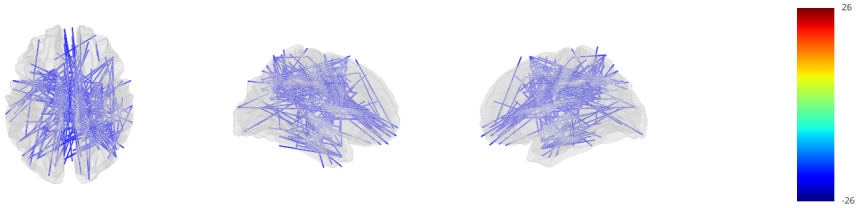

Fig. B.7. Changes in OAC in significant theta bin (Wilcoxon rank-sum, p<=1e-10)

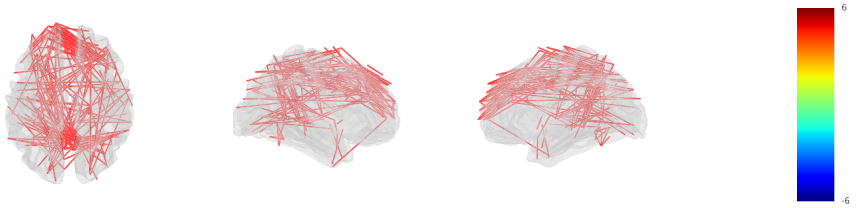

Fig. B.8. Changes in OAC in significant alpha bin (Wilcoxon rank-sum, p<=1e-10)

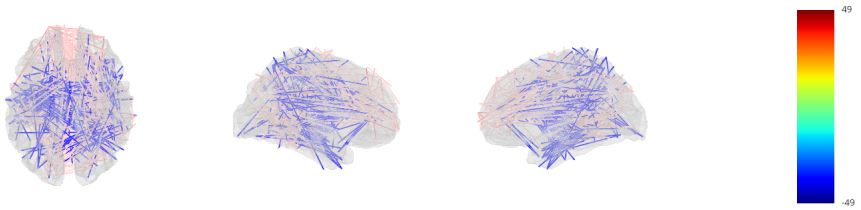

Fig. B.9. Changes in OAC in significant beta bin (Wilcoxon rank-sum, p<=1e-10)

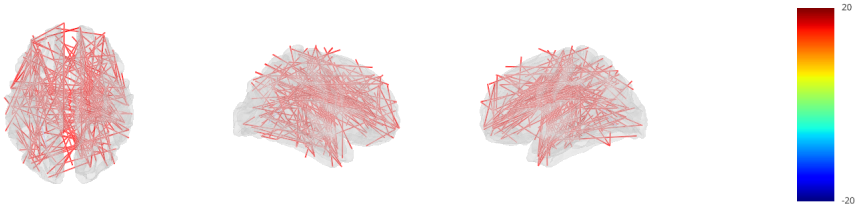

Fig. B.10. Changes in OAC in significant gamma bin (Wilcoxon rank-sum, p<=1e-10)

Annexe C

Sources-wise PAC changes in Frequency Clusters of Interest

C.1. Delta-alpha changes in PAC

C.2. Delta-beta changes in PAC

C.3. alpha-gamma changes in PAC

C.4. Delta-beta shift/reversal in PAC

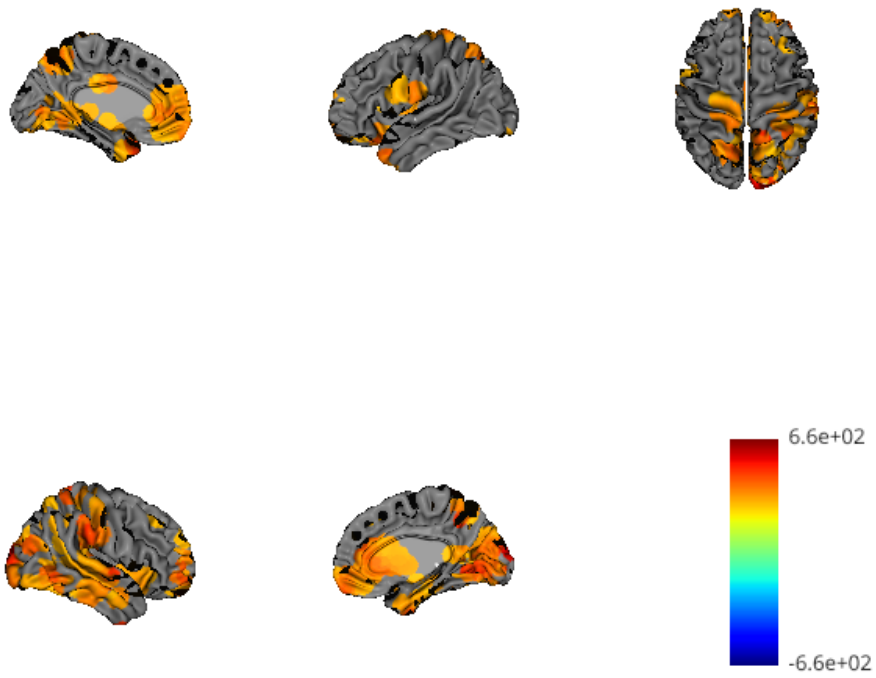

Fig. C.1. Amplitude source Increases in delta-alpha PAC cluster(Wilcoxon rank-sum, p<=1e-10)

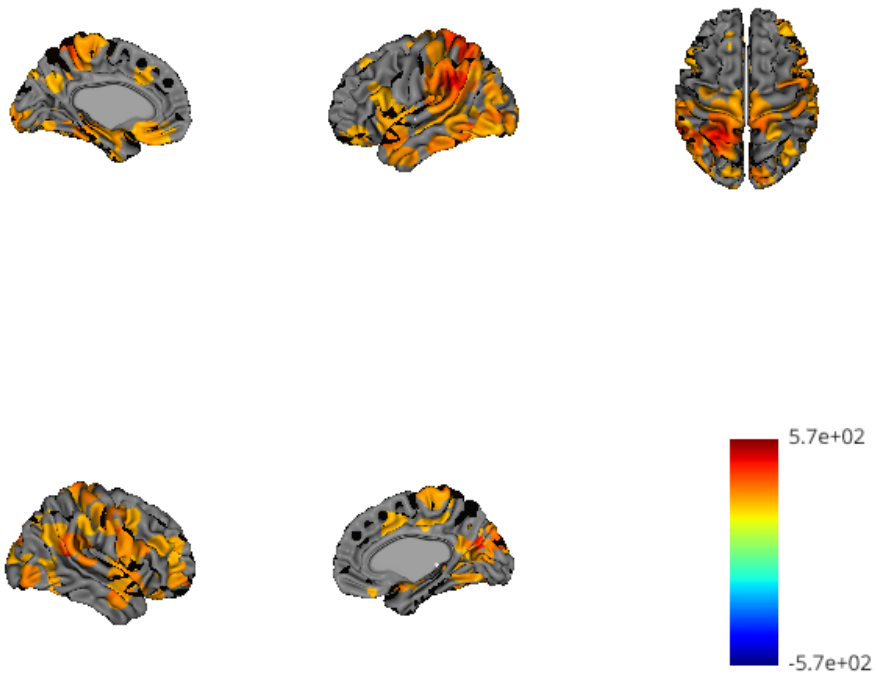

Fig. C.2. Phase source Increases in delta-alpha PAC cluster(Wilcoxon rank-sum, p<=1e-10)

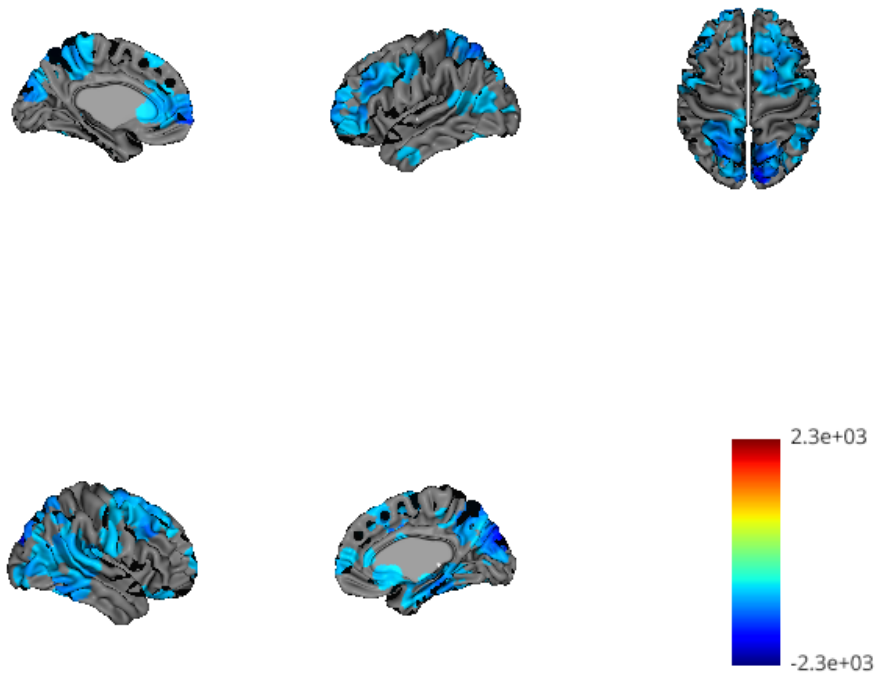

Fig. C.3. Amplitude source Decreases in delta-alpha PAC cluster(Wilcoxon rank-sum, p<=1e-10)

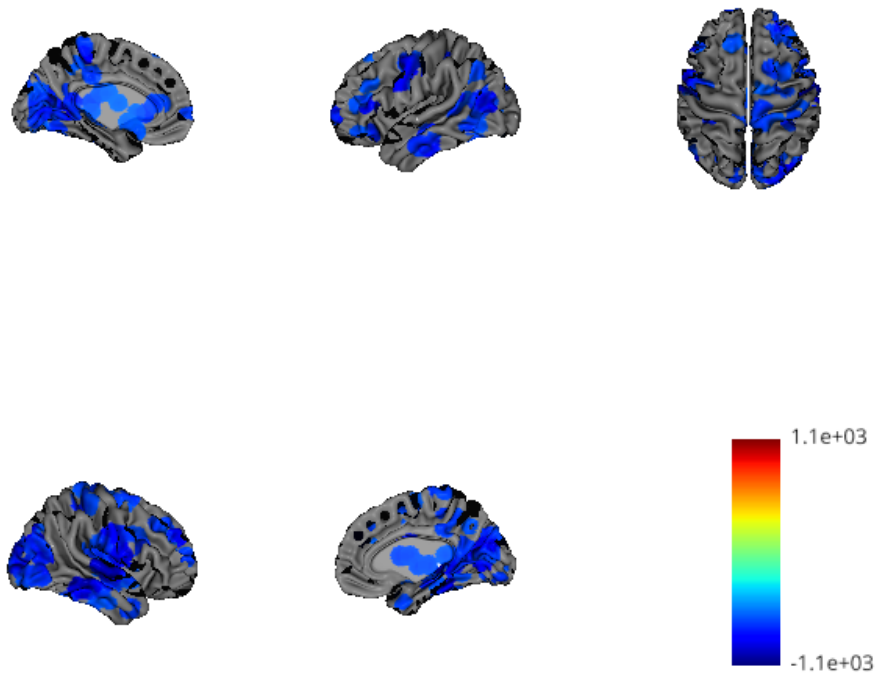

Fig. C.4. Phase source Decreases in delta-alpha PAC cluster(Wilcoxon rank-sum, p<=1e-10)

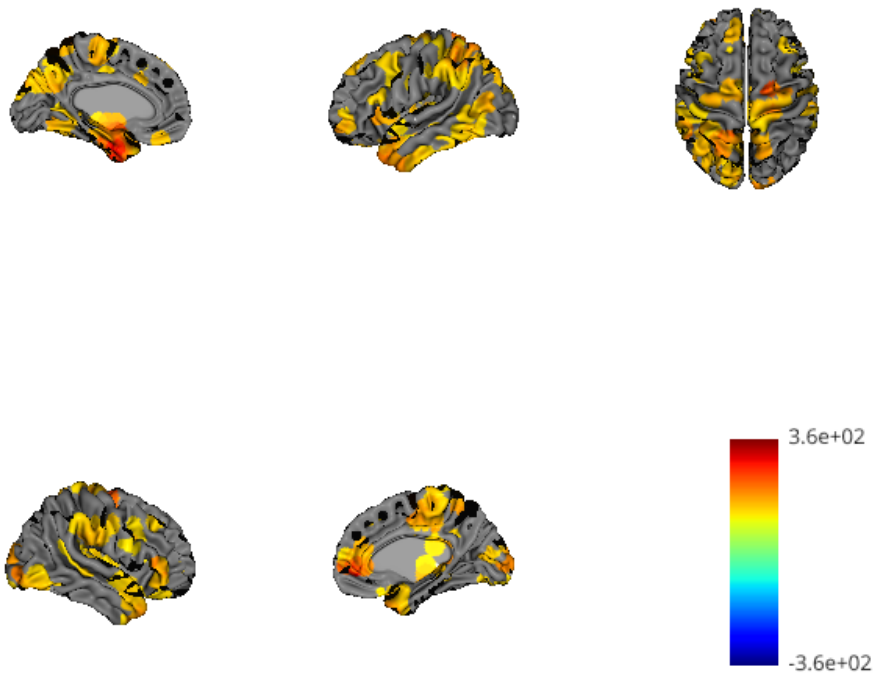

Fig. C.5. Amp source Increases in delta-beta PAC cluster(Wilcoxon rank-sum, p<=1e-10)

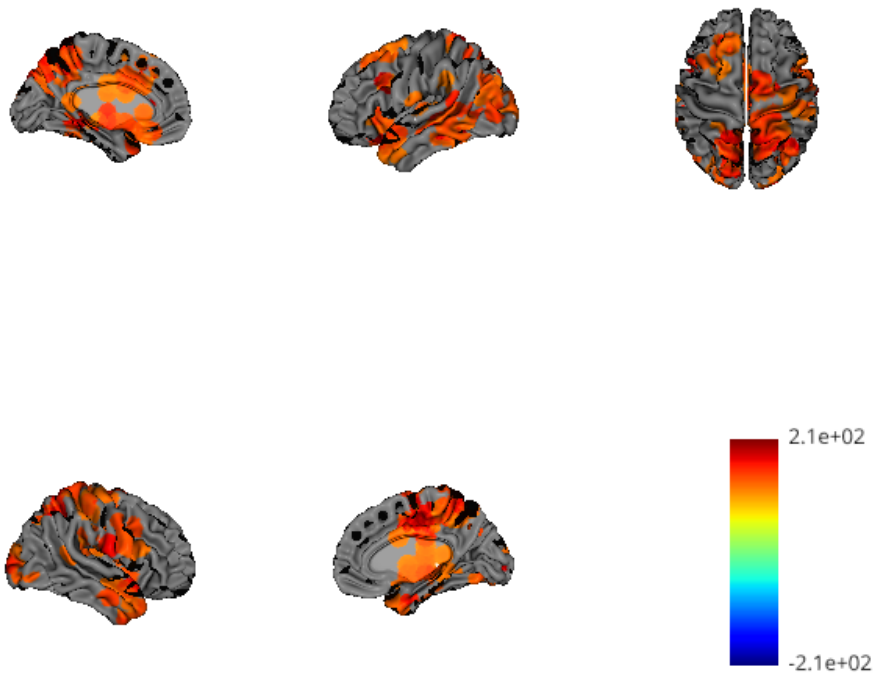

Fig. C.6. Phase source Increases in delta-beta PAC cluster(Wilcoxon rank-sum, p<=1e-10)

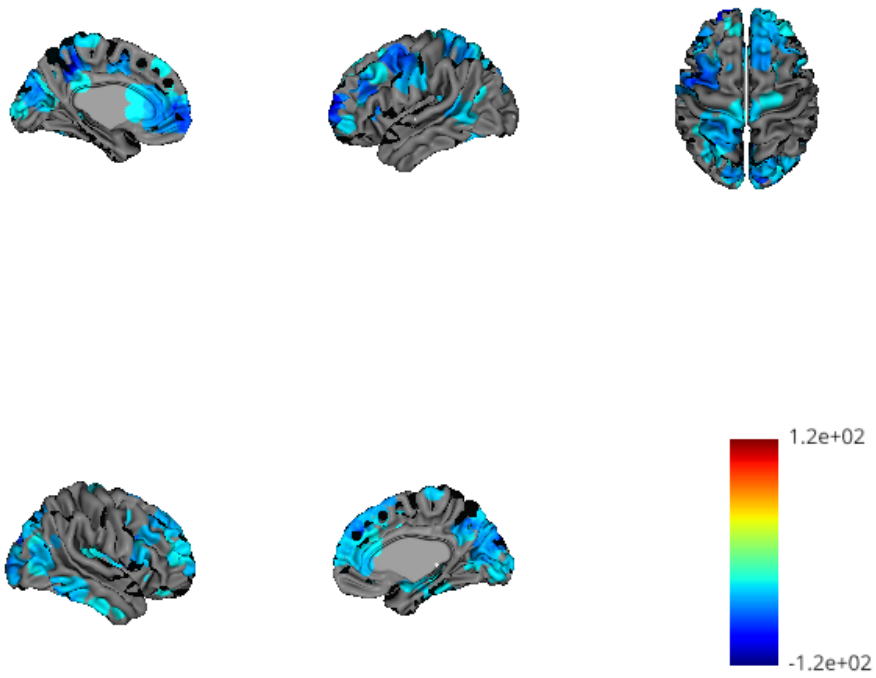

Fig. C.7. Amplitude source Decreases in delta-beta PAC cluster(Wilcoxon rank-sum, p<=1e-10)

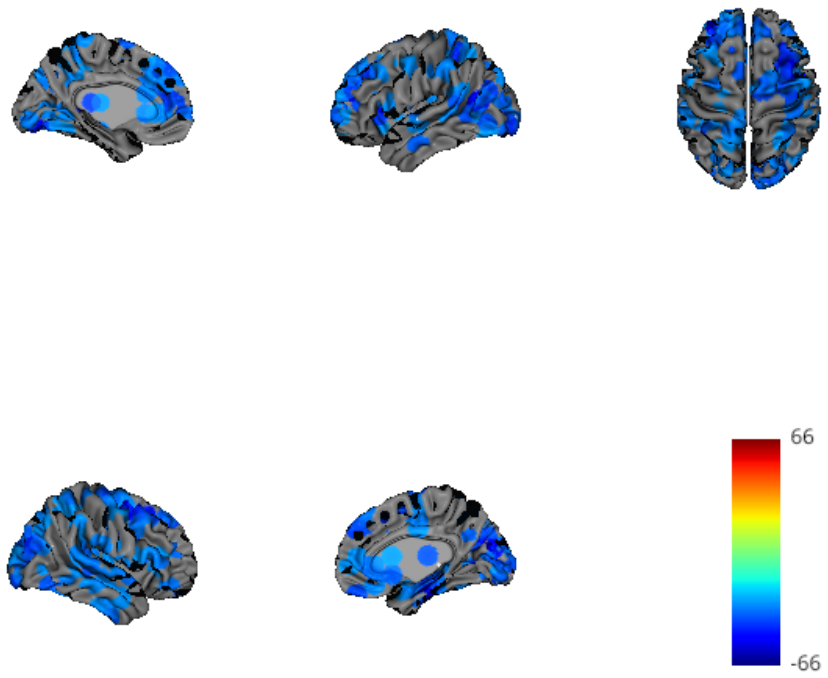

Fig. C.8. Phase source Decreases in delta-beta PAC cluster(Wilcoxon rank-sum, p<=1e-10)

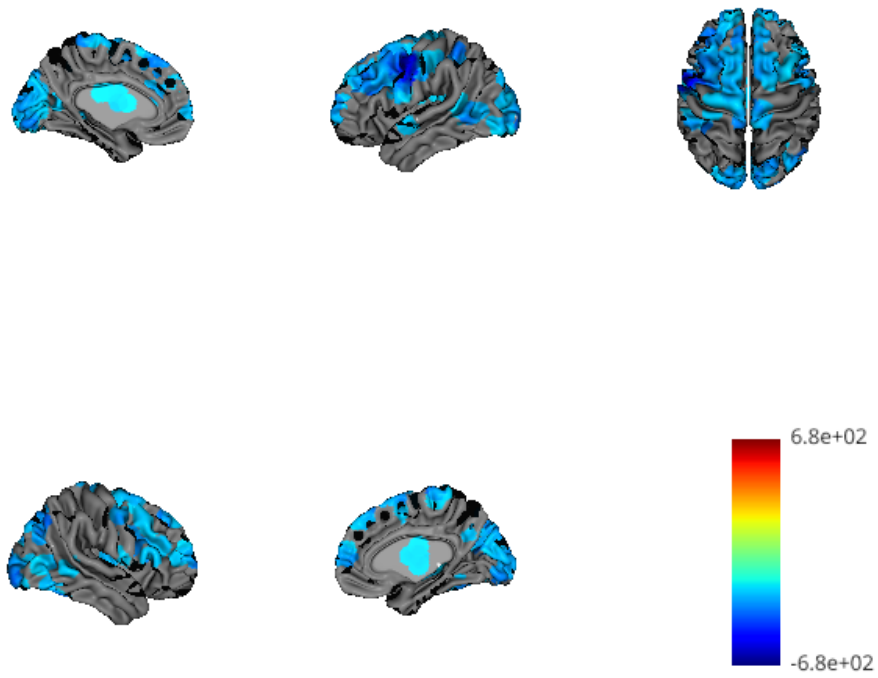

Fig. C.9. Amp source Decreases in alpha-gamma PAC cluster(Wilcoxon rank-sum, p<=1e-10)

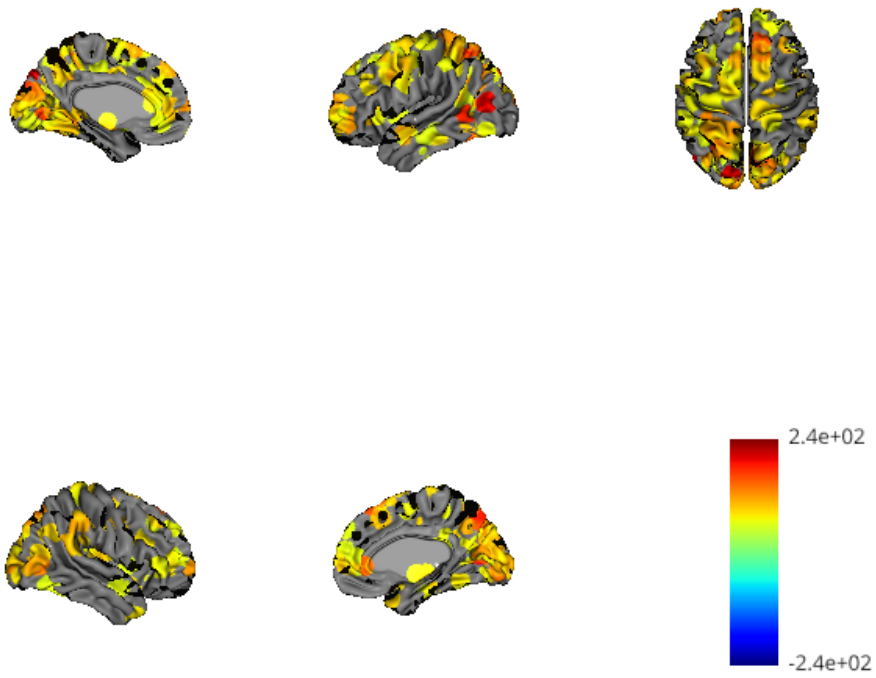

Fig. C.10. Amplitude sources reflecting frequency shift under LSD(Wilcoxon rank-sum, p<=1e-10)

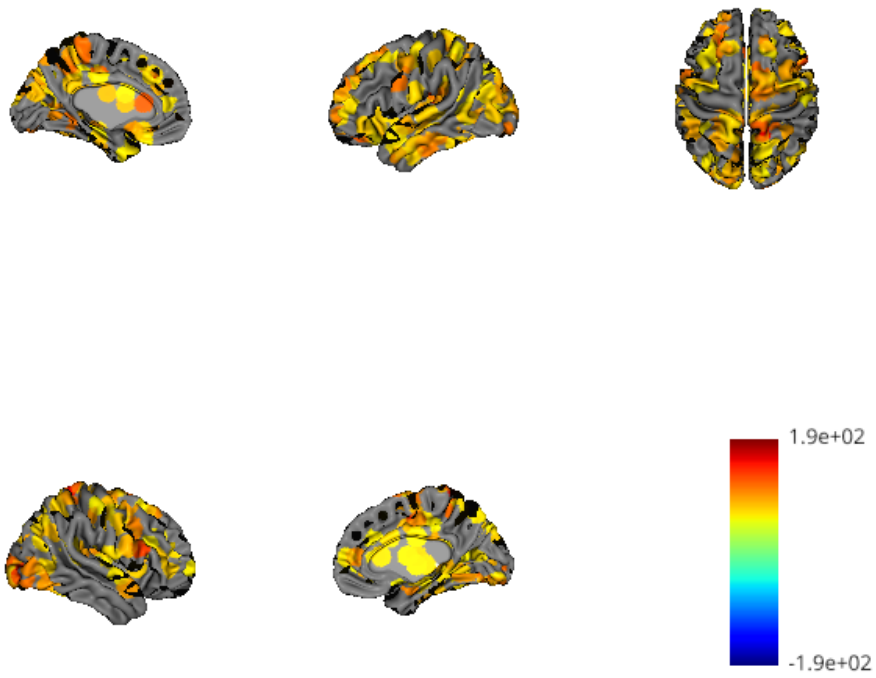

Fig. C.11. Phase sources reflecting frequency shift under LSD(Wilcoxon rank-sum, p<=1e-10)

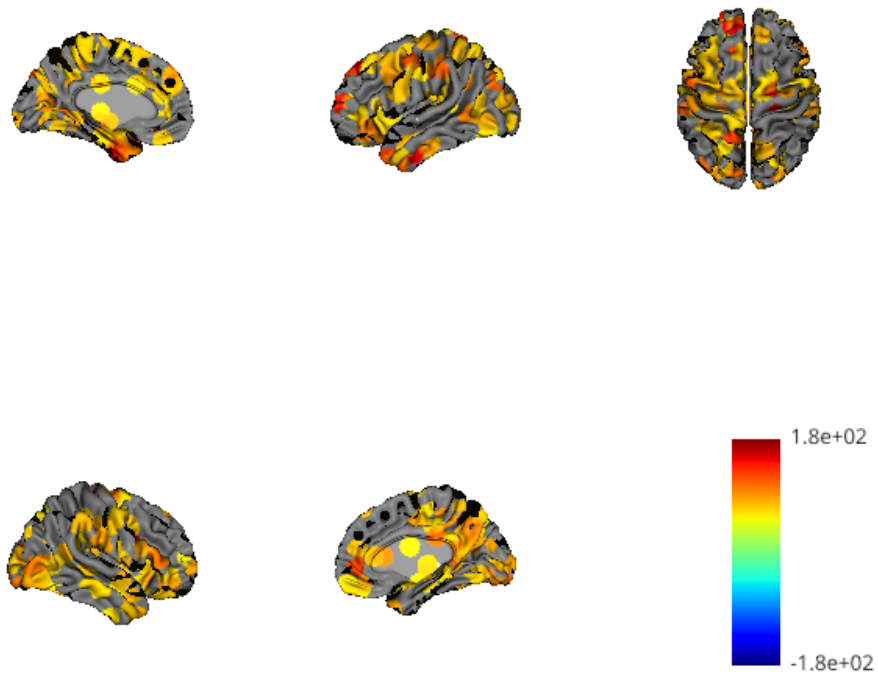

Fig. C.12. Phase source decreases where Amp sources increase in delta-beta PAC cluster(Wilcoxon rank-sum, p<=1e-10)

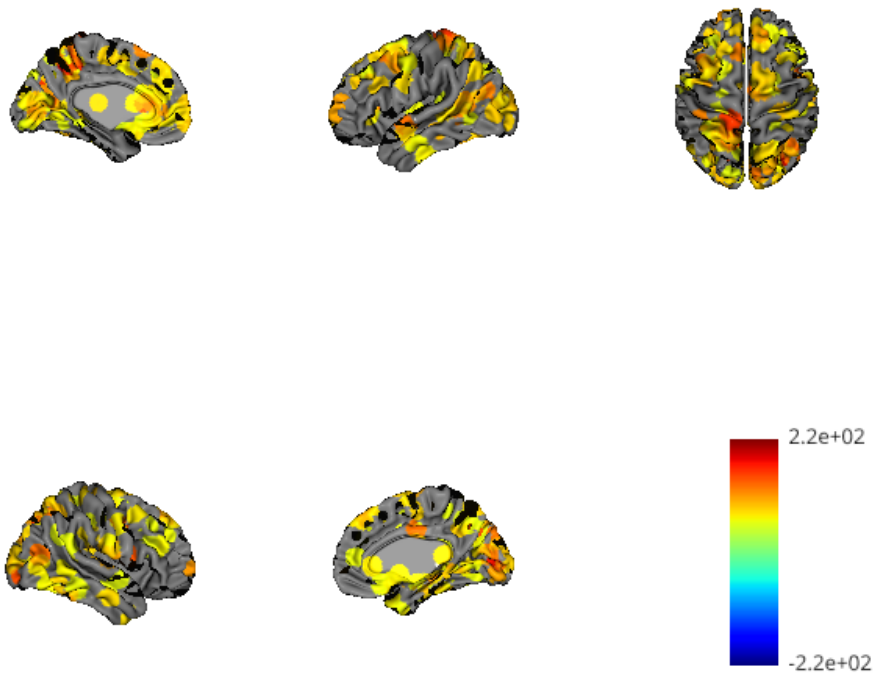

Fig. C.13. Amplitude source decreases where Phase sources increase in delta-beta PAC cluster(Wilcoxon rank-sum, p<=1e-10)